5-2-2022

Applying Data Mining Algorithms on Open Source Intelligence to Combat Cyber Crime

Xucan Chen

APPLYING DATA MINING ALGORITHMS ON OPEN SOURCE INTELLIGENCE TO COMBAT CYBER CRIME

by

XUCAN CHEN

Under the Direction of Yubao Wu, Ph.D.

ABSTRACT

In this dissertation, we investigate the applications of data mining algorithms on online criminal information. Ever since the entry of the information era, the development of the world wide web makes the convenience of peoples' lives to the next level. However, at the same time, the web is utilized by criminals for illegal activities like drug smuggling and online fraudulence. Cryptomarkets and instant message software are the most popular two online platforms for criminal activities. Here, we try to extract useful information from related open source intelligence in these two platforms with data mining algorithms.

Cryptomarkets (or darknet markets) are commercial hidden-service websites that operate on The Onion Router (Tor) anonymity network, which have grown rapidly in recent years. In this dissertation, we discover interesting characteristics of Bitcoin transaction patterns in cryptomarkets. We present a method to identify vendors' Bitcoin addresses by matching vendors' feedback reviews with Bitcoin transactions in the public ledger. We further propose a cost-effective algorithm to accelerate both steps effectively. Comprehensive experimental results have demonstrated the effectiveness and efficiency of the proposed method.

Instant message(IM) software is another base for these criminal activities. Users of IM applications can easily hide their identities while interacting with strangers online. In this dissertation, we propose an effective model to discover hidden networks of influence between members in a group chat. By transferring the whole chat history to sequential events, we can model message sequences to a multi-dimensional Hawkes process and learn the Granger Causality between different individuals. We learn the influence graph by applying an expectation–maximization(EM) algorithm on our text biased multi-dimensional Hawkes Process. Users in IM software normally maintain multiple accounts. We propose a model to cluster the accounts that belong to the same user.

INDEX WORDS: Bitcoin, Darknet, Submodular, Group Chat, Hawkes Process, Granger Causality, Representation Learning

APPLYING DATA MINING ALGORITHMS ON OPEN SOURCE INTELLIGENCE TO COMBAT CYBER CRIME

by

XUCAN CHEN

A Dissertation Submitted in Partial Fulfillment of the Requirements for the Degree of

Doctor of Philosophy

in the College of Arts and Sciences

Georgia State University

2022

APPLYING DATA MINING ALGORITHMS ON OPEN SOURCE INTELLIGENCE TO COMBAT CYBER CRIME

by

XUCAN CHEN

TABLE OF CONTENTS

LIST OF TABLES

LIST OF FIGURES

LIST OF ABBREVIATIONS

- IM - Instant Messaging
- TOR - The Onion Router
- NLP - Natural Language Processing
- CEAS- Cost Effective Addresses Searching
- HP - Hawkes Process
- TTMHP - Temporal Textual Multi-dimensional Hawkes Process
- EM - Expectation Maximization
- AHIN- Attributed Heterogeneous Information Network

PART 1

INTRODUCTION

Illegal online sales have grown exponentially [1]. Vendors can sell illicit products through cryptomarkets or encrypted IM messages software like telegram easily. In darknet, the privacy of participants in illicit online transactions is protected through both Tor and cryptocurrency. The darknet utilizes The Onion Router (Tor) network to hide users' IP addresses from the internet service provider. Darknet markets choose cryptocurrencies as payment currency mainly because they are anonymous. Unlike traditional currencies, cryptocurrencies like Bitcoin are decentralized[2]: there is no central authority responsible for the issuance of cryptocurrencies and there is no need to involve a trusted third-party like banks when making online transfers [3, 4]. Both buyers and vendors can trade anonymously through cryptocurrencies [5]. For IM software like telegram, they provide encryption services for users. Users of IM applications can easily hide their identities while interacting with strangers online. The privacy provided by darknet and IM software make it hard for law enforcement to trace illicit business online. This fact inspires us to conduct the research to extract useful information from public data in these platforms through data mining algorithms to combat cyber crime.

We first investigate the characteristics of Bitcoin transactions behind cryptomarkets in part 2. Darknet utilized the decentralized cryptocurrencies as payment currency. We conduct transactions on different types of markets to discover the currency management of cryptomarkets. In part 3, we further propose a method to identify vendors' Bitcoin addresses by matching vendors' feedback reviews with Bitcoin transactions in the public ledger. Each feedback review is matched to a Bitcoin transaction based on timestamp and value transferred in this transaction. Therefore a Bitcoin address whose history transactions can match more reviews of a vendor have a higher possibility to belong to this vendor. In part 4, we propose a model to discover hidden influence networks between members in a group chat. We can model message sequences to a Temporal-Textual Multi-Dimensional Hawkes process and learn the Granger Causality between different individuals. In part 5, we propose a model to cluster the accounts that belong to the same user in IM software. We design a 24-7 CNN to learn the representations of timestamp lists. By leveraging the post and time pattern of accounts, we propose a method to learn the embedding of each account and train a binary classifier to identify accounts from the same user.

1.1 Background

In this chapter, we provide the background information of our topic, including Darknet, Bitcoin, and Hawkes Process respectively.

1.1.1 Darknet

A darknet market is a commercial website on the dark web that operates via darknets such as Tor. They function primarily as black markets, selling or brokering transactions involving drugs, weapons, counterfeit currency, stolen credit card details, forged documents, unlicensed pharmaceuticals, steroids and other illicit goods as well as the sale of legal products. Tor is a network of virtual tunnels that allows you to improve your privacy and security on the Internet. Tor works by sending your traffic through three random relays in the Tor network. The last relay in the circuit (the “exit relay”) then sends the traffic out onto the public Internet. Tor provides hidden services (also known as onion services) for users to hide their locations and identities while offering web publishing services. Vendors and buyers can surf the darknet through Tor browser without leakage of their IP addresses to internet service providers.

1.1.2 Bitcoin

Bitcoin is the first decentralized cryptocurrency (also known as digital currency or electronic cash) that operates on the peer-to-peer network without the need for intermediaries and there are no central banks or administrators. Transactions are verified by network nodes via cryptography and recorded in a public distributed ledger called a blockchain. Users can transfer Bitcoin pseudonymously because funds are not tied to real-world entities but rather bitcoin addresses. Owners of bitcoin addresses are not explicitly identified. We focus on Bitcoin in this dissertation because Bitcoin is the most popular cryptocurrency which is accepted by all darknet markets [6]. Using blockchain and distributed ledger technology, the Bitcoin system promises great transparency and improved trust across transaction value chains [7, 8]. Without a third-party to ensure a transaction, the Bitcoin system publishes all of its history transaction data. The Bitcoin ledger stores all transaction records in history which are public to any Bitcoin users. A user wallet can own multiple bitcoin addresses, which are the "pseudonymous identity" of this user in the public ledger.

1.1.3 Hawkes Process

One-dimensional Hawkes process is a type of temporal point process which can model the self-exciting event sequence. The intuition behind it is that previous events may trigger the occurrence of future events. A temporal point process can be represented as a counting process, $N = \{N(t)|t \in [0, T]\}$, where $N(t)$ records the number of events before time t. Intensity function $\lambda(t) = \mathbb{E}[(dN(t)|H)]/dt$ represents the expected instantaneous happening rate of event given the event history H. Due to self-excitation, the intensity function of Hawkes process is conditionally based on history events. Given a sequence of n events on time $T = \{t_1, t_2, t_3 ... t_n\}$, officially the intensity function of event in Hawkes process is

$$\lambda(t) = \mu + \sum_{j:t_j<t} \alpha \cdot g(t - t_j) \tag{1.1}$$

where μ is exogenous base intensity independent of history while the second part on the right side is impact from previous events. t_j is the occurrence time of a previous event. $g(\Delta t)$ is the triggering kernel which decays with time difference. The earlier the previous event, the less impact it has on the current event. α is a coefficient measuring the amount of influence from previous events on the current event. Here we use an exponentially decaying function to capture the influence.

$$g(t_i - t_j) = \beta e^{-\beta(t_i - t_j)} \tag{1.2}$$

1.2 Characteristics of Bitcoin Transactions on Cryptomarkets

The darknet is a portion of the Internet that purposefully protects the identities and privacy of both web servers and clients. The Onion Router (Tor) is the most popular instance of a darknet and also the most popular anonymous network. A cryptomarket (or darknet market) is a commercial website operating on the darknet. Specifically, in Tor, a cryptomarket is a hidden service website with a ".onion" link address. Most products being sold in cryptomarkets are illicit. Some examples of popular products in cryptomarkets are drugs, malware, and stolen credit cards. After the demise of the first cryptomarket called Silk Road in 2013, new cryptomarkets have proliferated. Bitcoin is accepted in all cryptomarkets. As the first decentralized cryptocurrency, Bitcoin operates on the peer-to-peer network without the need for intermediaries and there are no central banks or administrators. In this section, we systematically study the vulnerabilities of Bitcoin privacy that exist in cryptomarkets. We identify and categorize patterns of Bitcoin transactions in cryptomarkets. The observations are then used for discussing the possibility of re-identifying Bitcoin addresses related to cryptomarkets. The conclusions obtained from this chapter can help design better Bitcoin payment systems and strengthen the privacy protection. On the other hand, the conclusions can also be used by law enforcement to understand the activities in cryptomarkets.

1.3 Identifying Darknet Vendor Wallets by Matching Feedback Reviews with Bitcoin Transactions

In part 3, we aim at finding vendors' Bitcoin addresses used in the darknet markets by matching feedback reviews with Bitcoin transactions. To narrow down the scope of the problem, we choose Bitcoin and Wall Street Market as a study example. Each feedback review is matched to a Bitcoin transaction based on timestamp and value transferred in this transaction. Specifically, we decompose our problem formulation into two sub-problems:

Bounding Box Matching Problem and Maximum Review Coverage Problem. In the Bounding Box Matching Problem, we construct a bounding box for each review and find matched Bitcoin transactions. We build a K-D tree from massive Bitcoin transaction data to achieve quick range searching in a bounding box. In the Maximum Review Coverage Problem, we prove the NP-Hardness of the problem. We exploit the submodular property of the objective function and design a greedy algorithm with an approximation ratio of $(1 - 1/e)$ to find a set of addresses that can cover near-optimal product reviews received by one vendor. Our method can discover the number of addresses used by one vendor, realizing one-to-many mapping. We further develop an algorithm that can effectively accelerate the matching and greedy algorithm.

Our contributions are as follows:

- We propose the problem of identifying the vendors' Bitcoin addresses by matching public Bitcoin transactions to vendor's feedback reviews in darknet markets. This problem is important because of two potential applications. First, it helps law enforcement to trace illicit transactions. Second, it reveals a privacy concern of cryptocurrencies so helps better design new cryptocurrencies.

- We decompose the complicated problem into two sub-problems and provide efficient computing algorithms for the sub-problems. We further propose a Cost-Effective Addresses Searching(CEAS) algorithm to accelerate the whole process, which can reduce about 60% matching calculations in experiments.

- We extensively evaluate our methods in both real and synthetic data and demonstrate the effectiveness and accuracy of our method.

1.4 Learning Infectivity Graph in Chat Group via Temporal Textual Multi-dimensional Hawkes Process

Instant message(IM) applications provide a convenient way for people to communicate and exchange confidential information. Users of IM applications can easily hide their identities while interacting with strangers online. To protect user's privacy, some IM developers provide encryption services for their customers. However, these privacy-protecting and convenient software has been utilized by criminals for illegal activities like drug smuggling, online fraudulence or even anti-social activities[9].

In part 4, we propose a framework which extracts the weighted directed infectivity graph by applying data mining and natural language processing techniques on the chat log of a group. The chat history is a sequence of messages where each message contains information including time when the message is posted, members who post the message and text content. The timestamp of each message makes chat history a time series data, which can be viewed as event sequences containing multiple event types and modeled via multi-dimensional point processes. Each posted message can be viewed as an event with a timestamp and the person's identity can represent the corresponding event type. To construct Granger Causality graph over event types(members in group), we model the data with a special class of point processes called Hawkes processes. Hawkes Process is a type of temporal point process which is widely used to model the self-exciting event sequences like earthquakes. When there are multiple event types, Hawkes Process is capable of describing mutually-triggering patterns among different event types. We relate influence between users to the possibility of replies among members. Natural language processing techniques are utilized to find dialogues in group chat logs. Impact functions of Hawkes process can capture the influence graph.

Our contributions are as follows:

- We propose the problem of detecting the influence graph from group chat. It helps law enforcement to analyze the organizational structure and key person from criminal activities in group chat.

- We present a modeling framework based on text biased Marked Multi-dimensional Hawkes Process. Hawkes Process can extract mutual-triggering patterns over individuals in a group. We further apply natural language processing techniques to identity conversations from the chat log and update impact functions of Hawkes process with the reply embedding. By applying an EM algorithm on the model, we are able to learn the influence graph over individuals from chat logs.

.

1.5 Clustering of Accounts in Online Messaging Software through Attributed Heterogeneous Information Networks

In this work, we propose a model to learn the representations of each account in group chat through attributed heterogeneous information networks.

The aim of this work is to cluster users based on time pattern and text of the post. The intuition behind our method is that if a vendor has several accounts, he or she will post the similar content with a similar time pattern by using these accounts.

Our contributions are as follows:

- We present a model to learn the representations of time stamp series by training a CNN auto-encoder. The embedding we learned can be used to measure the similarity of two timestamp lists effectively.
- We build an Attributed Heterogeneous Information Network. In the AHIN we built, it contains four types of nodes: User, account, post and product. We train a model to learn the embedding of each node. To effectively measure the relationship between nodes in constructed AHIN, we sample paths from AHIN through weighted random walk and propose a new network embedding model User2Vector to learn the hidden representations of each user. We further train a binary classifier to classify two user representations we learned by User2Vector.
- We extensively evaluate our methods in both real and synthetic data and demonstrate the accuracy of our method.

1.6 Proposed Dissertation Organization

In this dissertation proposal, we plan to investigate how to efficiently extract useful information from darknet and IM software. In part 2, we describe our experiments of purchases in cryptomarkets and summarize the Bitcoin transaction mechanisms behind cryptomarkets. In part 3, we present a greedy method to identify vendors' bitcoin addresses by matching vendors' feedback reviews with Bitcoin transactions in the public ledger. In part 4, we present our work which models group chat with Hawkes Process to discover hidden networks of influence between members. In part 5, we propose a model to cluster the accounts from the same user by learning the embedding of these accounts. In part 6, we conclude this dissertation.

PART 2

CHARACTERISTICS OF BITCOIN TRANSACTIONS ON CRYPTOMARKETS

In this chapter, we discover interesting characteristics of Bitcoin transaction patterns in cryptomarkets. The results demonstrate that the privacy protection mechanism in cryptomarkets and Bitcoin is vulnerable.

2.1 Motivation

Illegal online sales have grown exponentially [1]. The privacy of participants in illicit online transactions in darknet is protected through both Tor and cryptocurrency. Vendors in cryptomarket sell illicit products like drugs, malware, and stolen credit cards. The sales on the darknet market hit a new high in 2021 although the law enforcement has spent a lot of resources to fight these illegal transactions.

Table (2.1) Cryptomarkets and Accepted Cryptocurrencies

Cryptomarkets	#Ads	Bitcoin	Monero	Litecoin	Ethereum	Bitcoin Cash
Dream	$166,216$	✓				✓
Berlusconi	$38,462$	✓				
Wall Street	$16,847$	✓	✓			
Empire	$9,538$	✓	✓	✓		
Point Tochka	$6,468$	✓			✓	✓
Silk Road 3.1	$5,738$	✓	✓	✓	✓	

From Table 2.1, we can see that Bitcoin is accepted in all cryptomarkets. In addition to Bitcoin, four other types of cryptocurrencies are also accepted by different markets. They are monero, litecoin, ethereum, and Bitcoin cash. Note that Bitcoin cash is a variant of but different from Bitcoin and is an independent currency. Bitcoin cash is generally considered to be faster in the transaction confirmation process but less secure than Bitcoin. In our study, we focus on Bitcoin since it is the most popular cryptocurrency and widely accepted by all markets. The observed Bitcoin transaction patterns in this chapter provide insights for analyzing other types of cryptocurrencies.

Since all Bitcoin transactions are public, it is hard to fully protect the privacy of Bitcoin users. The news has revealed that adversaries could spy on a careless company by first paying it in Bitcoins and then tracking how that money flows [10–12]. To better protect the privacy, Bitcoin users have extensively used mixing services to obscure the Bitcoin trails [10].

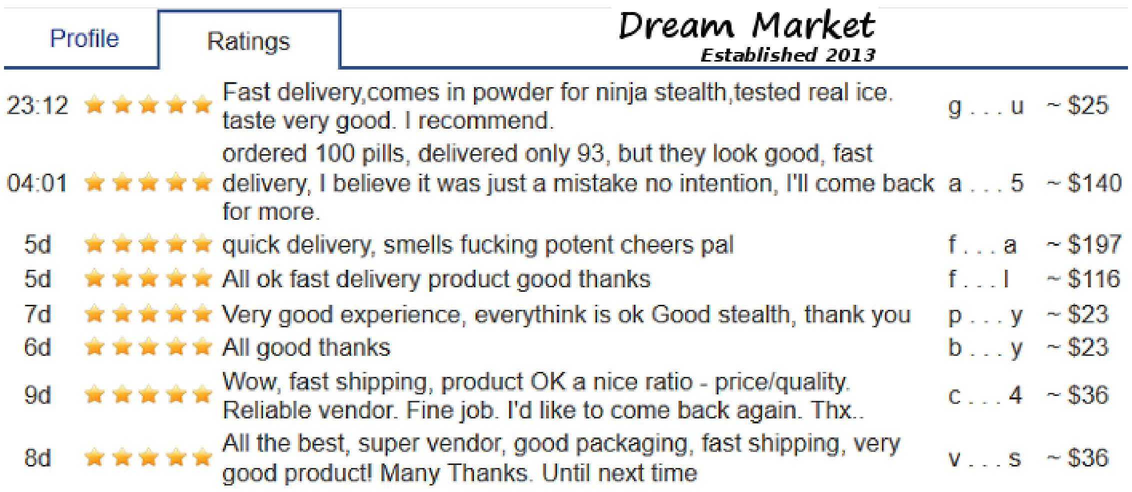

23:12	★★★★★	Fast delivery,comes in powder for ninja stealth,tested real ice. taste very good. I recommend.	g . . . u	~ $25
04:01	★★★★★	ordered 100 pills, delivered only 93, but they look good, fast delivery, I believe it was just a mistake no intention, I'll come back for more.	a . . . 5	~ $140
5d	★★★★★	quick delivery, smells fucking potent cheers pal	f . . . a	~ $197
5d	★★★★★	All ok fast delivery product good thanks	f . . . l	~ $116
7d	★★★★★	Very good experience, everythink is ok Good stealth, thank you	p . . . y	~ $23
6d	★★★★★	All good thanks	b . . . y	~ $23
9d	★★★★★	Wow, fast shipping, product OK a nice ratio - price/quality. Reliable vendor. Fine job. I'd like to come back again. Thx..	c . . . 4	~ $36
8d	★★★★★	All the best, super vendor, good packaging, fast shipping, very good product! Many Thanks. Until next time	v . . . s	~ $36

Figure (2.1) The Feedback in the Dream Market

In cryptomarkets, adversaries could place orders and then track money flows. Cryptomarkets display the buyers' feedback in order to demonstrate the vendors' reputation. Figure 2.1 shows the screenshot of the feedback page in the Dream Market. From Figure 2.1, we can see the post time, rating star, text comment, masked buyer ID, and approximate amount of money. Each rating actually represents a Bitcoin transaction. Even though we can only observe approximate time and money in ratings, the accumulation of a lot of such approximate transaction records could potentially allow adversaries to reveal relevant Bitcoin addresses. Figure 2.2 shows the screenshot of the feedback page in the Wall Street Market. From Figure 2.2, we can observe similar ratings. All markets in Table 2.1 display feedback publicly. This potentially allows adversaries to re-identify the Bitcoin addresses of buyers, vendors, and escrow accounts in cryptomarkets, thus increasing the vulnerability of

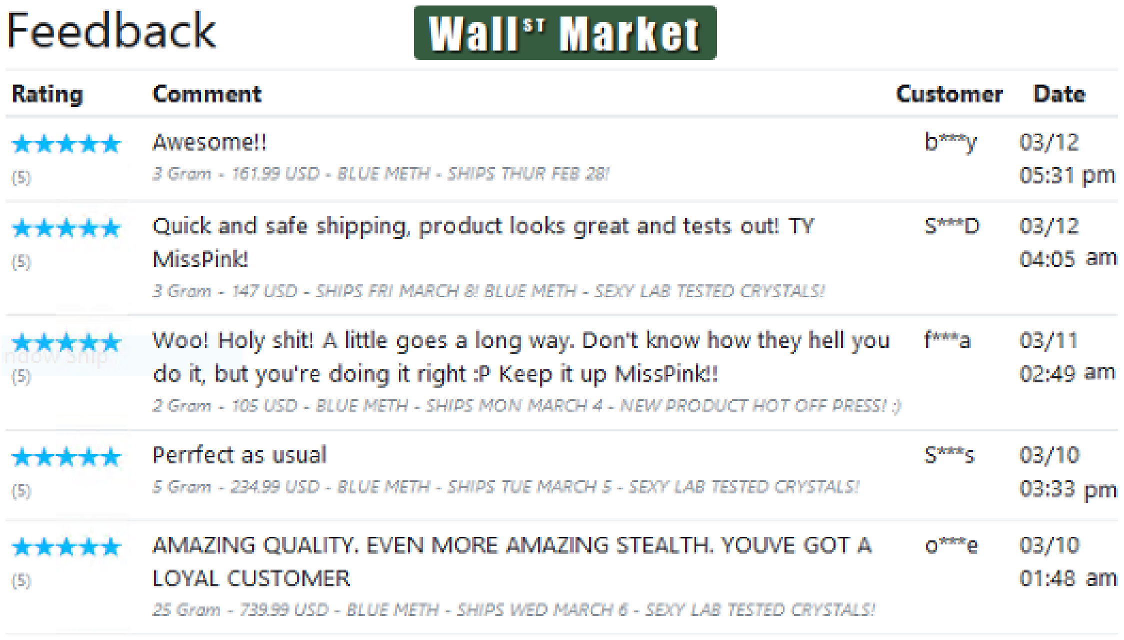
Feedback

Wall^ST Market

Rating	Comment	Customer	Date
★★★★★ (5)	Awesome!! *3 Gram - 161.99 USD - BLUE METH - SHIPS THUR FEB 28!*	b***y	03/12 05:31 pm
★★★★★ (5)	Quick and safe shipping, product looks great and tests out! TY MissPink! *3 Gram - 147 USD - SHIPS FRI MARCH 8! BLUE METH - SEXY LAB TESTED CRYSTALS!*	S***D	03/12 04:05 am
★★★★★ (5)	Woo! Holy shit! A little goes a long way. Don't know how they hell you do it, but you're doing it right :P Keep it up MissPink!! *2 Gram - 105 USD - BLUE METH - SHIPS MON MARCH 4 - NEW PRODUCT HOT OFF PRESS! :)*	f***a	03/11 02:49 am
★★★★★ (5)	Perrfect as usual *5 Gram - 234.99 USD - BLUE METH - SHIPS TUE MARCH 5 - SEXY LAB TESTED CRYSTALS!*	S***s	03/10 03:33 pm
★★★★★ (5)	AMAZING QUALITY. EVEN MORE AMAZING STEALTH. YOUVE GOT A LOYAL CUSTOMER *25 Gram - 739.99 USD - BLUE METH - SHIPS WED MARCH 6 - SEXY LAB TESTED CRYSTALS!*	o***e	03/10 01:48 am

Figure (2.2) The Feedback in the Wall Street Market

the privacy protection in Bitcoin.

2.2 Related Work

Ron et al. is the first to build a Bitcoin graph and analyze the quantitative attributes in Bitcoin transaction history [13]. Clustering Bitcoin addresses into wallets is one basic task in the Bitcoin transaction analysis. Researchers have widely used two simple heuristics [14–16]. The first heuristic is to put shadow or change address together with its input address into one wallet. The second heuristics is to put all input addresses into one wallet if there is a single output address. Androulaki et al. test the effectiveness of the Bitcoin address clustering methods with stimulations [14]. Spagnuolo et al. link the clustered wallets to the Silk Road escrow addresses exposed by FBI and analyze the Bitcoin flow [15]. Fleder et al. not only link the clustered wallets with Silk Road escrow but also link wallets with public wallets [16]. PageRank is then applied on the transaction graph to find interesting and important wallets [16]. The effectiveness of address clustering is also studied [17]. Mixing technology is also introduced to improve the anonymity [18, 19].

2.3 Escrow Services in Cryptomarkets

In this section, we review the escrow services in cryptomarkets. All cryptomarkets provide escrow services to avoid scams and protect both buyers and vendors.

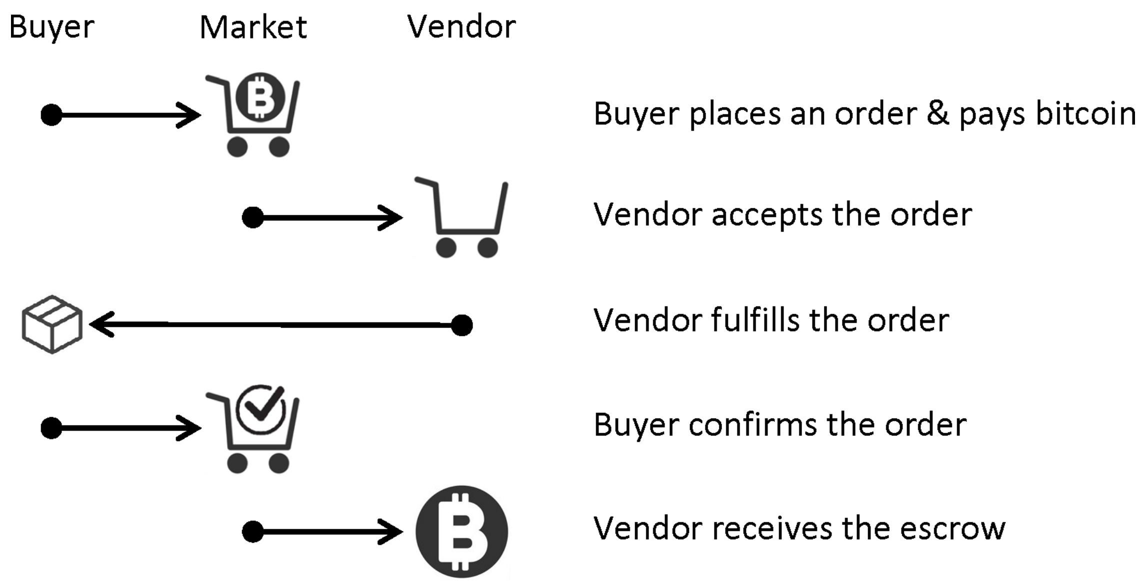
Buyer
Market
Vendor
Buyer places an order & pays bitcoin
Vendor accepts the order
Vendor fulfills the order
Buyer confirms the order
Vendor receives the escrow

Figure (2.3) A Flowchart Depicting a Transaction in Cryptomarkets

Figure 2.3 shows the typical process of one transaction [20]. The buyer places an order and pays with Bitcoins after browsing the products within the Tor web browser. The market holds the Bitcoins until the buyer confirms the order. The vendor accepts and fulfills the order. The buyer confirms the order and gives feedback reviews. The market releases the Bitcoins to the vendor and charges a commission fee. If the buyer is not satisfied with the product or service, the buyer disputes the order. In this case, the market decides where the escrow Bitcoins go. The escrow Bitcoins go either back to the buyer or to the vendor depending on the dispute result.

2.4 Bitcoin Transactions

2.4.1 Parsing Bitcoin Transactions

To trace the Bitcoin flow, we parse the blocks in the public Bitcoin blockchain and obtain the Bitcoin transactions. We install the Bitcoin core program [21] and run a Bitcoin full node [22]. The Bitcoin full node automatically synchronizes with other nodes in the Bitcoin network, and downloads all blocks in the blockchain. The blocks contain the public ledger data and are the inputs of our parsing algorithm. A new block is generated around every 10 minutes.

Algorithm 1 Parsing Bitcoin Transactions

Input: Blocks in the Bitcoin blockchain

Output: Bitcoin transactions (a set of .json files whose names are formatted timestamps)

```
for each block do
    transaction_time ⇐ block.timestamp;
    create a new file: formatted_transaction_timestamp.json;
    for each transaction in the block.transactions do
        transaction_hash ⇐ transaction.this_transaction_hash;
        receiver_list = [] ;
        for each receiver in the transaction.receivers do
            receiver_list.add(receiver.index, receiver.Bitcoin_address, receiver.Bitcoin_value)
        sender_list = [] ;
        for each sender in the transaction.senders do
            sender_list.add(sender.index, sender.previous_transaction_hash,
              sender.previous_transaction_index)
        [transaction_time, transaction_hash, sender_list, receiver_list] ⇒
          formatted_transaction_timestamp.json
```

Algorithm 1 shows our parsing algorithm. We use the existing Python Bitcoin parser to parse the blocks (raw Bitcoin data) and construct the Bitcoin transaction tree [23, 24]. In Algorithm 1, we parse the blocks one by one (lines 1-12) and save one timestamp for all transactions in one block (line 2). For each transaction in one block, we parse the transaction hash (line 5), the receiver list (lines 6-8), and the sender list (lines 9-11). Each transaction contains four parts: timestamp, hash, sender_list, and receiver_list, and is written into a

Algorithm 2 Constructing Bitcoin Transaction Flow Tree

Input: Bitcoin transactions (a set of .json files whose names are formatted timestamps)

Output: Bitcoin transaction flow tree $G(V, E)$

```
read the list of json files;
for each json file (process them in the chronological order) do
    read all transactions in the json file;
    for each transaction tx do
        for each receiver in tx.receiver_list do
            add node $r$ = [tx.transaction_hash, receiver.index, receiver.Bitcoin_address,
              receiver.Bitcoin_value] to the node set $V$;
            for each sender in tx.sender_list do
                find node $s \in V$ with $s$.transaction_hash = sender.previous_transaction_hash
                  and $s$.index = sender.index;
                add an edge $(s, r)$ to the edge set $E$;
```

json file (line 12). One receiver contains the Bitcoin address and the Bitcoin values. Each sender in one transaction does not contain a Bitcoin address nor Bitcoin value. Instead, each sender contains transaction hash and index pointing to an earlier transaction. We can use that transaction hash to retrieve the earlier transaction and use the transaction index to find the referred receiver from the receiver list. By linking the sender in the current transaction with the receiver in the earlier transaction, we can generate a Bitcoin transaction flow tree.

Algorithm 2 shows the construction of the Bitcoin transaction flow tree. Algorithm 2 processes the json files in the chronological order. This guarantees that old transactions will be processed earlier than new transactions. Since a receiver has a Bitcoin address, we can directly add a node (transaction_hash, Bitcoin_address) to the flow tree. Since a sender does not have a Bitcoin address, we need to look it up in an earlier transaction. Since earlier transactions have been processed, the sender must exist in the node set V as a receiver. Therefore, we search over all the nodes in V and compare the transaction_hash and index values (lines 8). Then we add an edge from this earlier receiver to the current receiver in the flow tree. If there are multiple senders and receivers in a mixing transaction, these senders and receivers will form a complete bipartite graph, i.e., there is an edge from any sender to any receiver. We do not know who sends money to whom in a mixing transaction.

Algorithm 3 Local Search Algorithm for Extracting a Subtree

Input: Bitcoin transaction flow tree $G(V, E)$, query $q = (q\_hash, q\_btc\_address)$, k hops

Output: Subtree $G[T]$

```
ignore the edge direction, $G.Adj[u]$ represents the neighbors;
for each node $v \in V$ do $v.d = \infty$ ;
$S \Leftarrow \{q\}$; $T \Leftarrow \{\}$; $q.d = 0$;
while True do
    extract node $u$ with minimum $u.d$ value among all nodes in the set $S - T$;
    if $u.d > k$ then break;
    $T \Leftarrow T \cup u$; $S \Leftarrow S \cup G.Adj[u]$;
    for each node $x$ in $G.Adj[u]$ do $x.d = \min\{x.d, u.d + 1\}$ ;
```

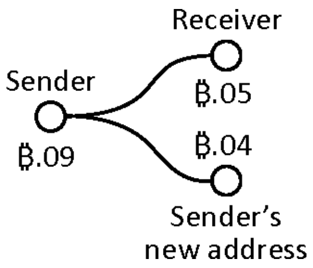

Figure (2.4) Shadow Address

Algorithm 3 shows a local search algorithm that retrieves a subtree containing all nodes that are k-hop away from the query node. The query node is determined by the transaction hash and Bitcoin address. In our experiment, we use Algorithm 3 to extract a subtree given a query node containing our Bitcoin address. The subtree is nimble for us to analyze interesting patterns.

Shadow Address: Bitcoin creates a new address for the sender in each transaction to obtain better anonymity [25]. The newly generated address is called "shadow address" or "change address" of the original address of the sender [14]. Figure 2.4 shows one Bitcoin transaction. The sender's original address has .09. After .05 is sent to the receiver, the sender still has .04 in the change address.

Multiple inputs and single output: Considering the multiple addresses one user can own, Bitcoin supports a user to send Bitcoins from multiple addresses in one transaction. Figure 2.5 shows one Bitcoin transaction containing multiple inputs and one output. The sender sends money from four Bitcoin addresses to the receiver's address. We assume that it is unlikely that two senders send money to the same address at the same time since the Bitcoin addresses keep changing. If we observe a transaction with multiple inputs and single output, we can assume all input addresses belong to the same sender.

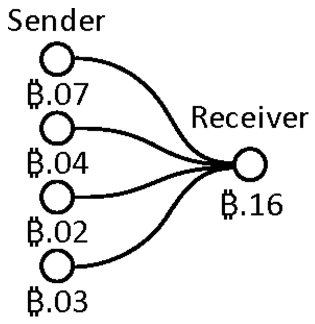

Figure (2.5) Multi-Inputs

These two properties help track Bitcoin flows or cluster addresses into wallets [14, 16, 26].

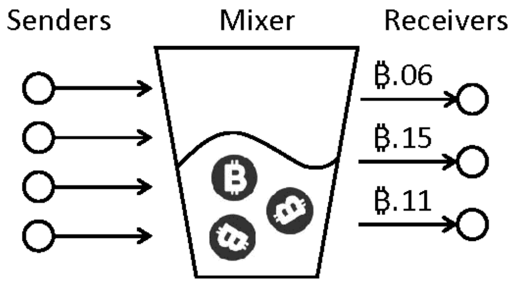

Figure (2.6) A Mixing Transaction

Mixing services: are widely used as a privacy overlay on top of Bitcoin [27]. Mixing services are also known as tumblers. The mixer will mix several transactions into one, intending to confuse the trail linking back to the source. In a mixing transaction, the multiple inputs are from different senders and the multiple outputs go to different receivers. Mixing services reduce the traceability of Bitcoin flows which makes the analysis of Bitcoin graphs more difficult. Figure 2.6 shows a mixing transaction with four senders and three receivers. In this example, we do not know who sends money to whom because there are multiple possible flows.

2.4.2 Actions and Observed Resulting Transactions

In this section, we describe our experiments in cryptomarkets. All cryptomarkets offer escrow services to avoid scams. With the escrow service, the Bitcoin is saved in escrow accounts after a buyer places an order and is sent to the vendor until the buyer confirms the order. Since we know the start point (buyer address) of the transaction, we can trace Bitcoin flows to uncover escrow and vendors' addresses.

Table (2.2) Observed Bitcoin Flow from Operations in Different Cryptomarkets

Cryptomarkets	Deposit	Withdraw	Order	Confirm
Point Tochka	✓	✓	✓	✓
Dream	✓	✓	No observation	No observation
Empire	✓	✓	No observation	No observation
Silk Road 3.1	✓	✓	No observation	No observation
Wall Street	No such function	No such function	✓	✓
Berlusconi	No such function	No such function	✓	No observation

In each market, four operations are performed: deposit, withdraw, order, and confirmation. The resulting transactions may or may not be observed in the Bitcoin transaction flow. Table 2.2 shows whether we can observe the Bitcoin transactions for the four operations in cryptomarkets. From Table 2.2, we can see that the Dream, Empire, and SilkRoad 3.1 Market operate in a similar way. These markets require buyers to deposit Bitcoins first. When buyers withdraw Bitcoins from the market, the market will send Bitcoins to buyers' wallets from an address different from the deposit address. When we order or confirm a purchase, we cannot observe any transactions in Bitcoin flow. The Point Tochka Market also requires a deposit. When we order and confirm a purchase in the Point Tochka Market, we can observe the transactions from buyer to escrow and then to vendor in the Bitcoin flow. The Wall Street and Berlusconi Markets do not require deposit. In the Wall street Market, when we order and confirm a purchase, we can also observe the corresponding transactions in the Bitcoin flow. In the Berlusconi Market, we can observe the transactions in Bitcoin flow when we order. The Bitcoins sent to escrow are transferred to other escrow addresses through a mixing service before we confirm the purchase. Therefore, we cannot observe the transaction when we confirm the purchase.

Table (2.3) Deposit and Withdrawal in the Point Tochka Market

Action	Observed Bitcoin transaction		Balance
	Sender	Receiver	
Deposit .0024	A1: .0030	B1: .0024, A2: .0006	.0024
Withdraw .0008	B1: .0024	A2: .0008, B1: .0016	.0016
Deposit .0010	A2: .0006, A2: .0008	B1: .0026, A3: .0004	.0026
Withdraw .0006	B1: .0026	A3: .0006, B1: .0020	.0020

In the next, we will study the Bitcoin transaction patterns when we interact with the markets. We first study the deposit and withdrawal actions and then the order and confirmation actions. In each market, four operations are performed: deposit .0024, withdraw .0008, deposit .0010, and withdraw .0006. We monitor the Bitcoin transaction flow to see whether we can observe any related transactions or not. To simplify the illustration, we omit the fees charged during the deposit and withdrawal actions.

Deposit and Withdrawal in the Point Tochka Market: Table 2.3 shows the actions we perform and the resulting Bitcoin transactions in the Point Tochka Market. In Table 2.3, each row represents an action we perform and the resulting Bitcoin transaction. We use letter "A" followed by an integer to represent our Bitcoin addresses and letter "B" followed by an integer to represent the deposit Bitcoin addresses provided by the market.

For example, in the first row, we deposit .0024 and the resulting transaction is "A1: .0030 $\rightarrow$ B1: .0024, A2: .0006". In the sender part "A1: .0030", A1 represents our Bitcoin address and .0030 represents the money in that address. In the receiver part "B1: .0024, A2: .0006", B1 represents the deposit Bitcoin address provided by the Point Tochka Market, .0024 represents the money that B1 receives, A2 represents our new Bitcoin address, and .0006 represents the change in the new address A2. The last column in Table 2.3 shows the balance in the market wallet.

In the second row of Table 2.3, we withdraw .0008 and the resulting transaction is "B1: .0024 → A2: .0008, B1: .0016". B1 still represents the deposit Bitcoin address and A2 still represents our Bitcoin address for receiving the money. We further deposit .0010 and withdraw .0006, and the resulting transactions are shown in Table 2.3.

From Table 2.3, we can see that the deposit Bitcoin address in the market does not change. Among all cryptomarkets in Table 2.1, the Point Tochka Market has the most transparent Bitcoin transaction flows, which can be further confirmed when we study the order and confirmation actions.

Table (2.4) Deposit and Withdrawal in the Dream Market

Action	Observed Bitcoin transaction		Balance
	Sender	Receiver	
Deposit .0024	A1: .0030	B1: .0024, A2: .0006	.0024
Withdraw .0008	B2: .0008	A2: .0008	.0016
Deposit .0010	A2: .0006, A2: .0008	B3: .0010, A3: .0004	.0026
Withdraw .0006	B4: .0006	A4: .0006	.0020

Deposit and Withdrawal in the Dream Market: We perform the same sequence of actions in the Dream Market and Table 2.4 shows the resulting transactions. From Table 2.4, we can see that the Bitcoin address B2 that sends us money during the first withdrawal is different from the Bitcoin address B1 that receives our money during the first deposit. After the second withdrawal, we find that there is still .0024 in B1. This means that the Dream Market uses different Bitcoin addresses to receive deposits and send withdrawal. From the subsequent deposit and withdrawal actions, the deposit is sent to B3 and the withdrawal is received from B4. This further confirms the observation. This mechanism makes it harder to track the Bitcoin flow, thus better protects the privacy of the market and prevents the re-identification attack.

The Empire and Silk Road 3.1 Markets have similar transaction patterns as Dream Market for the deposit and withdrawal actions. We omit the tables for them. The Wall

Street and Berlusconi Markets provide neither deposit nor withdrawal functions. They allow buyers to directly pay from their own Bitcoin addresses.

In the next, we study patterns in the resulting Bitcoin transactions for the order and confirmation actions.

Table (2.5) Order and Confirmation in the Point Tochka Market

Action	Observed Bitcoin transaction		Balance
	Sender	Receiver	
Order .0014	B1: .0040	C1: .0014, B1: .0026	.0026
Confirm	C1: .0014	D1: .0014	.0026
Order .0015	B1: .0026	C2: .0015, B1: .0011	.0011
Confirm	C2: .0015	D2: .0015	.0011

Order and Confirmation in the Point Tochka Market: We purchase two orders and Table 2.5 shows the resulting Bitcoin transactions. After we place the first order, the money is sent from the deposit Bitcoin address B1 to an escrow account C1. The balance is sent back to B1. After the vendor fulfills the order, we confirm it. The money in the escrow C1 is then immediately transferred to a new Bitcoin address D1, which is suspected of being the vendor's Bitcoin address. In the second order, we pay 0.0015 to a different vendor. Similar to the transactions in the first order, the money moves to an escrow account C2 after the order and then moves from C2 to the destination Bitcoin address after confirmation. The escrow address C2 is different from the old escrow address C1. From this experiment, we can see that the Bitcoin transaction flows are transparent. For each new order, the market will generate a new escrow Bitcoin address. We also observe that our deposit Bitcoin address will not change. By tracking the money flowing out of the escrow accounts, we can potentially find the suspicious Bitcoin addresses of vendors.

Order and Confirmation in the Dream Market: We also purchase two products in the Dream Market and Table 2.6 shows the resulting transactions. After we place the first order of 0.0014, we find that no transaction associated with the deposit Bitcoin address

Table (2.6) Order and Confirmation in the Dream Market

Action	Observed Bitcoin transaction		Balance
	Sender	Receiver	
Order .0014	B1: .0040 does not change		.0026
Confirm	B1: .0040 still no change. No transactions observed		.0026
Order .0015	B1: .0040 does not change		.0011
Confirm	B1: .0040 still no change. No transactions observed		.0011

B1 happens. After the vendor fulfills the order and we confirm it, still nothing happens. This means Dream Market uses a different escrow Bitcoin address to pay the vendor and the money in the original deposit address B1 does not move. Since we know neither the escrow address used to pay the vendor nor the vendor Bitcoin address, there is no easy way for us to observe the relevant transactions. We suspect that the Dream Market has its own private ledger to record the balances of the deposit and escrow accounts for each user. After each order, the Bitcoin in the deposit account will be transferred to the escrow account. After each confirmation, the Bitcoin in the escrow account will be transferred out to the vendor's accounts. The ledger of Dream Market might be a private and centralized ledger. This strategy makes the transactions within the Dream Market stealthy and cannot be seen from the public. This strategy well protects the privacy of the market and vendors.

Table (2.7) Order and Confirmation in the Wall Street Market

Action	Observed Bitcoin transaction	
	Sender	Receiver
Order .0014	A1: .0040	C1: .0014, A2: .0026
Confirm	C1: .0014 is transferred to another address through mixing	
Order .0015	A2: .0026	C2: .0015, A3: .0011
Confirm	C2: .0015 is transferred to another address through mixing	

Order and Confirmation in the Wall Street Market: The Wall Street Market does not have a deposit function. It allows us to pay directly with our Bitcoin address. When we purchase, we are required to send a specific amount of Bitcoin to a newly generated escrow address and to provide a Bitcoin address for receiving the refund if the order fails. Following this procedure, we purchase two products. Table 2.7 shows the resulting transactions. After we place the first order, we can see the escrow address C1. After we confirm the order, we can observe that the money in the escrow C1 is transferred to a new Bitcoin address through a mixing service. Since there are multiple receivers, we do not know which one is the receiver corresponding to the escrow C1.

Table (2.8) Order and Confirmation in the Berlusconi Market

Action	Observed Bitcoin transaction	
	Sender	Receiver
Order .0014	A1: .0040	C1: .0014, A2: .0026
Confirm	C1: .0014 is transferred to another address through mixing	
Order .0015	A2: .0026	C2: .0015, A3: .0011
Confirm	C2: .0015 is transferred to another address through mixing	

Order and Confirmation in the Berlusconi Market: The Berlusconi Market does not have a deposit function either. We directly pay with our Bitcoin address and Table 2.8 shows the resulting transactions. After we place the first order, we can see the escrow address C1. But before we confirm the order, the money in the escrow C1 is already transferred to a new Bitcoin address through the mixing service. This makes it hard for us to track the Bitcoin flows. Similar pattern is observed for the second order. The Berlusconi Market applies mixing services on escrow addresses to further protect the privacy of the market and vendors.

Since the Wall Street and Point Tochka Markets provide more transparent Bitcoin transaction patterns, the feedback reviews may help re-identify the Bitcoin addresses of vendors. A feedback review is usually posted right after the buyer confirms the order. Each review represents an approximate Bitcoin transaction including approximate date and money. We will see more details in the next sections.

2.5 Bitcoin Transaction Patterns

2.5.1 Dream Market

In this section, we track back the Bitcoin flows of the withdrawal operation in Dream Market with Algorithm 3. We find a Bitcoin address containing more than 800 Bitcoins which is worth over 3 million dollars at present, and it collects those Bitcoins from multiple addresses in one transaction. Figure 2.7 shows part of the flow tree we observed. The red node represents our Bitcoin address for receiving money in the withdrawal. We observe a Bitcoin transaction pattern called "peeling chain" [26].

Peeling Chain: The head of a peeling chain is a Bitcoin address with a lot of Bitcoins. A small amount of Bitcoin is peeled off from this address in a transaction and a "Shadow address" is generated to collect the remaining and still large amount of Bitcoin. By repeating this process, the large amount of Bitcoin can be peeled down. Peeling chain is popular for organizations dealing with a lot of clients. The Bitcoin addresses in a peeling chain are not necessarily the addresses of Dream escrow accounts. They might be exchange addresses [28].

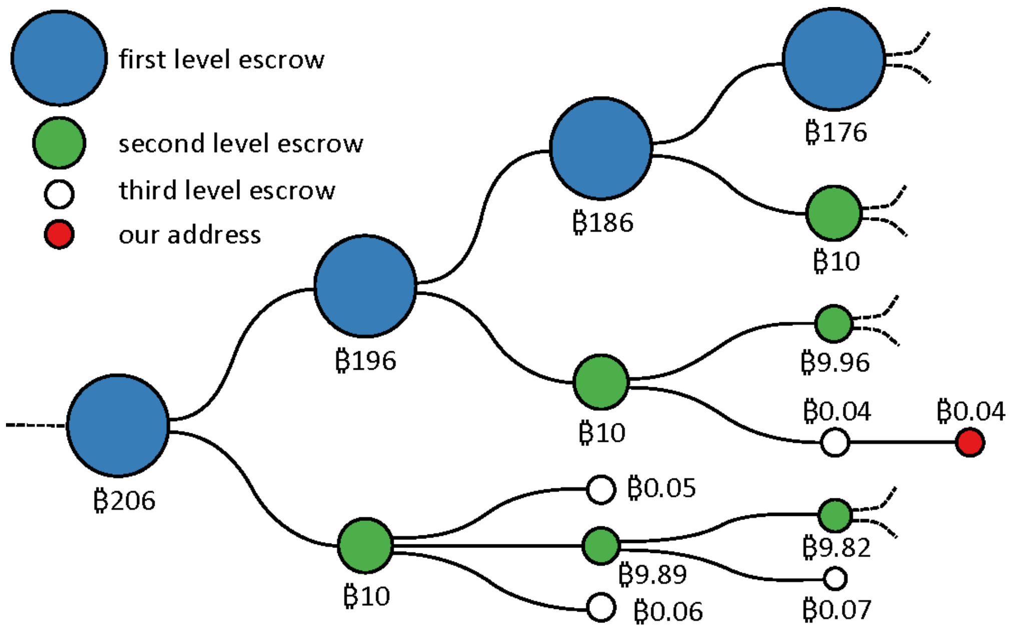

Figure (2.7) Bitcoin "peeling chain" Patterns in the Dream Market

The head of this peeling chain is a Bitcoin address which receives more than 800 Bitcoins. In each transaction, 10 Bitcoins are transferred to a new address and the remaining amount is transferred to the shadow address. We call these blue addresses in the main chain the first level escrow addresses. Each of the addresses containing 10 Bitcoins becomes a head of a new smaller peeling chain. In this new chain, one transaction peels off an even smaller amount of Bitcoin to pay different users. We call the green addresses in the smaller peeling chains the second level escrow addresses. The Bitcoins peeled off from the second order addresses are sent to third level escrow addresses, which are white nodes in Figure 2.7. The white nodes directly send Bitcoins to users (red nodes) of the dream market. The amount of Bitcoin received by the third order escrow address is exactly the number of Bitcoins required by users. No shadow addresses are generated.

In addition to this pattern, we also notice that the mixing pattern from the third order escrow addresses to users' addresses. The Dream market allows users to use mixing services. Users need to pay a certain percentage of fees to use mixing services when they withdraw Bitcoins.

Clustering Bitcoin addresses: The peeling chain patterns can potentially help cluster Bitcoin addresses of users in the Dream Market. Since we can track the peeling chain easily, we may be able to identify other transactions happening in the Dream Market by comparing the white-red transactions with the feedback reviews.

2.5.2 Wall Street Market

Table (2.9) The Bitcoin Transaction Relevant to the Order Action

Hash (txid)	25f33135c87b37205b49a9ade6faa1d6837a4fcb42340270753562b7e1802bee		
Time (UTC)	2019-03-05 16:49 Input count: 1 ; Output count: 2		
Input 0	`15v3cQR4H9iz3nb1tXwNd33ETo7ZEX2wir`	.03554909	$132.31
Output 0	`33sYgQnBkBkm3mDbWJY6KMoT7no1eNd4j5`	.00032256	$1.20
Output 1	`14ZKcens6g6J58kBVGNk3Hs2a94NE3bnUT`	.03517496	$130.92

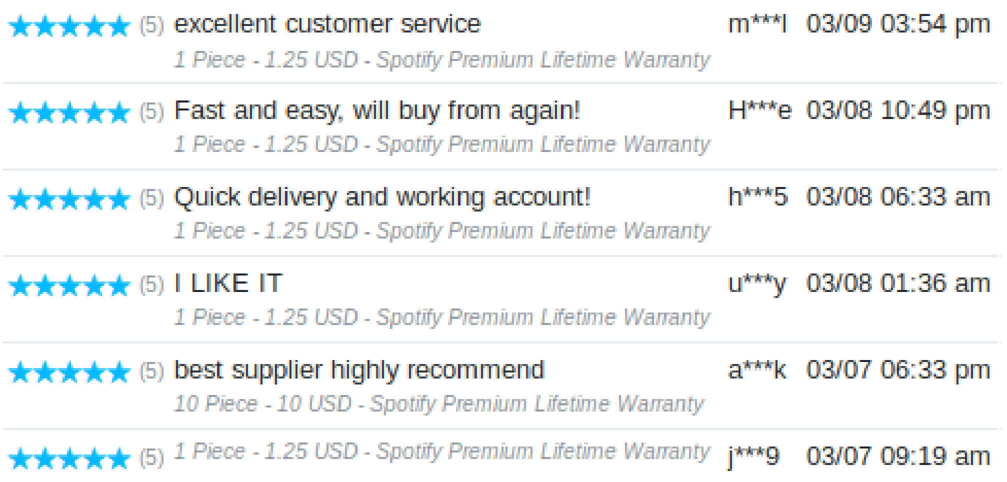

★★★★★ (5) excellent customer service m***l 03/09 03:54 pm
1 Piece - 1.25 USD - Spotify Premium Lifetime Warranty

★★★★★ (5) Fast and easy, will buy from again! H***e 03/08 10:49 pm
1 Piece - 1.25 USD - Spotify Premium Lifetime Warranty

★★★★★ (5) Quick delivery and working account! h***5 03/08 06:33 am
1 Piece - 1.25 USD - Spotify Premium Lifetime Warranty

★★★★★ (5) I LIKE IT u***y 03/08 01:36 am
1 Piece - 1.25 USD - Spotify Premium Lifetime Warranty

★★★★★ (5) best supplier highly recommend a***k 03/07 06:33 pm
10 Piece - 10 USD - Spotify Premium Lifetime Warranty

★★★★★ (5) 1 Piece - 1.25 USD - Spotify Premium Lifetime Warranty j***9 03/07 09:19 am

Figure (2.8) Feedback Ratings in the Wall Street Market

Table (2.10) The Bitcoin Transaction Relevant to the Confirmation Action

Feedback	u***y - 03/08 01:36 am - 1.25 USD		
Hash (txid)	27c4946ad1e5e648e987d66a882d98f08ebcb3bae8d11aea70b9dac7219aa036		
Time (UTC)	2019-03-08 02:06 Input count: 24 ; Output count: 22		
Input 16	33sYgQnBkBkm3mDbWJY6KMoT7no1eNd4j5	.00032256	$1.20
Output 8	39o2XAjmFTkSGFrkUPsJRNrDUvUCYiXyP5	.00061720	$2.39
Output 10	336djQeGFA4etdRv3xRESoKVV3zHr8YvMv	.00020500	$0.79
Output 18	3JppEPMTeUXWY96g5D19k6hhK1QLATdwJV	.00029320	$1.14

In this section, we explore the possibility of linking Wall Street feedback reviews with Bitcoin transactions. We order a product "Spotify Premium Lifetime Warranty" and pay $1.25 on about 4:40 pm, March 5, 2019, then we confirm the order and write a review by 01:36 am, March 8, 2019. Figure 2.8 shows some feedback reviews. In Figure 2.8, the fourth review is written by us and "u***y" is our account ID. Since we know our Bitcoin address "15v3...", we track the money flow.

Table 2.9 shows the transaction relevant to the order action. The output address "33sY..." is the escrow account, and the other output address "14ZK..." is the shadow address containing our remaining money. Table 2.10 shows the transaction relevant to the confirmation action. It is a mixing transaction containing 24 inputs and 22 outputs. The

Table (2.11) The Bitcoin Transactions Relevant to the Feedback Reviews in Fig. 2.8

Feedback	H***e - 03/08 10:49 pm - 1.25 USD		
Hash (txid)	5542aaf1c045f951ba7623510237217d97009eb403778cec6ae101d4462583e1		
Time (UTC)	2019-03-08 23:07 Input count: 47 ; Output count: 42		
Output 40	`3JppEPMTeUXWY96g5D19k6hhK1QLATdwJV`	.00028800	$1.12
Feedback	h***5 - 03/08 06:33 am - 1.25 USD		
Hash (txid)	bb6a4c9d5c747d941eeb6fc5031973351382cb0550be35bfbefda0c07380b63d		
Time (UTC)	2019-03-08 08:26 Input count: 15 ; Output count: 20		
Output 19	`3JppEPMTeUXWY96g5D19k6hhK1QLATdwJV`	.00029290	$1.13
Feedback	a***k - 03/07 06:33 pm - 10 USD		
Hash (txid)	c022177c6bb26a2c3ad82b699bb9d3d950131a8b13dd54665e7f6e4f8d8263a3		
Time (UTC)	2019-03-07 19:21 Input count: 35 ; Output count: 38		
Output 26	`3JppEPMTeUXWY96g5D19k6hhK1QLATdwJV`	.00251950	$9.75

escrow address “33sY...” is in the sender list. Table 2.10 shows top three output addresses whose receiving Bitcoins are most close to the money we send. By comparing the Bitcoins of the three outputs with our money $1.25, we can see that output address “3Jpp...” is most likely to be the vendor’s address. We can also see that the transaction happens at 2019-03-08 02:06, which is 30 minutes later than our review time 01:36 am.

We further explore the transactions related to “3Jpp...”. Table 2.11 shows the list of transactions relevant to the reviews in Figure 2.8. For example, the first transaction happens at 2019-03-08 23:07 and the amount of money is $1.12, which matches with the feedback review “H***e - 03/08 10:49 pm - 1.25 USD”. The time of the transaction is 18-minute later than the time of review. Comparing the reviews in Figure 2.8 with the transactions in Table 2.10 and 2.11, we can see we successfully find the transactions of four reviews. For the first and sixth reviews in Figure 2.8, we do not find them manually. This is because the vendor may have multiple Bitcoin address for receiving money and “3Jpp...” might be just one of them.

We purchase the product again and find the same Bitcoin address “3Jpp...” receiving the money. This further confirms that “3Jpp...” belongs to the vendor.

2.6 Conclusion

In this chapter, We find interesting Bitcoin transaction patterns associated with cryptomarkets. The results demonstrate that the privacy protection mechanism in Bitcoin is still vulnerable in terms of simple analysis. An adversary can easily gain valuable information for analyzing the activities happening in the markets.

PART 3

IDENTIFYING DARKNET VENDOR WALLETS BY MATCHING FEEDBACK REVIEWS WITH BITCOIN TRANSACTIONS

In this chapter, we extend our work to present a method to identify vendors' Bitcoin addresses by matching vendors' feedback reviews with Bitcoin transactions in the public ledger.

3.1 Motivation

In part 2, we describe our experiments of purchases in Wall Street market, the most popular darknet markets before it was taken down. Since we know the start point (buyer address) of the transaction, we can track Bitcoin flows from the start point during our purchase.

In darknet markets, buyers do not send Bitcoin to vendors directly. All darknet markets provide escrow services to avoid scams and protect both buyers and vendors. In each market, two operations are performed by the buyer: order and confirm the order. Like normal online shopping, buyers need to order products first and they can confirm this order once they receive the product. In part 2, we show whether we can observe related Bitcoin transactions in public ledger for these two operations in some biggest darknet markets [29]. In the Wall Street Market, when we order a product or confirm this order, a related Bitcoin transaction occurs .

Figure 3.1 shows the resulting Bitcoin flow during these two operations by a buyer. A consumer needs to send Bitcoin to a newly generated escrow address after he places an order. Bitcoin will stay in this escrow address until the buyer confirms the order when they received the product. The confirmation will trigger the Bitcoin transfer from the escrow address to the vendor's address through a mixed transaction. Mixed transactions are utilized to break the

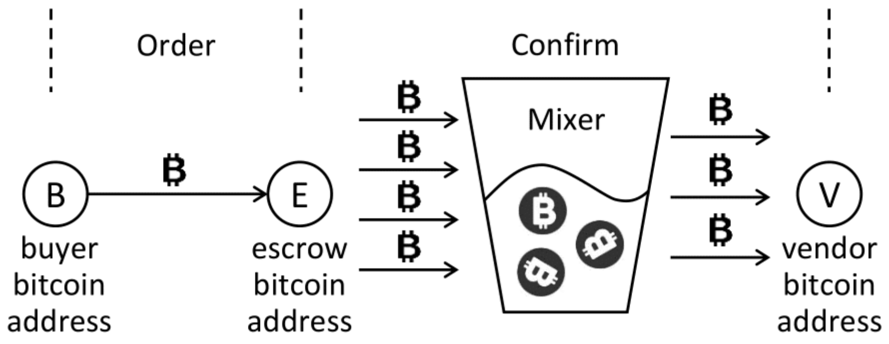

Figure (3.1) Bitcoin Flow of One Purchase in Wall Street Market

direct connection between the sender and receiver address by combining several transactions into one transaction with multiple senders and multiple receivers [30, 31]. However, we still can get the amount of Bitcoin received by each receiver address in mixed transaction.

In Wall Street Market, 94.5% of Bitcoin in escrow address is sent to the vendor's address, and the remaining 5.5% is transferred to the Wall Street market address as a commission fee during a mixed transaction. When the buyer confirms that they have received the illicit product, they need to write feedback that appears in the review list of products with time and amount of dollars spent during this transaction. Experiments we have in Wall Street Market show the time when the review posted is close to the time when a mixed transaction happened and the price of a product should be close to the Bitcoin value received by the vendor's address. Each feedback review is matched to a Bitcoin transaction based on timestamp and value transferred in this transaction. If we could find the related Bitcoin transaction in the public ledger, the receiver of this transaction is the Bitcoin address from the vendor.

3.2 Related Work

3.2.1 Bitcoin De-anonymization

The rise of Bitcoin has increased researchers' interest in privacy provided in cryptocurrency [32–36], also the usage of Bitcoin in darknet [37]. To attack the privacy of Bitcoin, the most common way is to study the Bitcoin transaction graph after clustering the Bitcoin address from one wallet. A wallet represents an entity. A user stores all addresses in a wallet. Researchers have widely clustered Bitcoin addresses heuristically. Androulaki tested the effectiveness of the Bitcoin address clustering methods with simulation [34]. Spagnuolo links the clustered addresses to the Silk Road escrow address exposed by the FBI and analyzes the Bitcoin flow related to this escrow address [32]. Fleder not only linked the clustered addresses to Silk Road escrow but also linked Bitcoin addresses to some public entities [33]. PageRank is then applied on the transaction graph to find addresses that are close to the Silk Road escrow address. In the transaction graph, each node represents an entity that contains all addresses owned by this entity. However, current clustering methods don't work for mixed transactions that combine several transactions into one transaction with multiple senders and multiple receivers. Mix is quite common in Bitcoin transactions, especially illegal transactions in recent years. In this chapter, our method is the first one to explore relationships between feedback of vendors and receiver parts of Bitcoin transactions which won't be affected by mixed transactions.

3.2.2 Matching

If we treat each review as one type of node and Bitcoin transaction as another type of node, reviews of a vendor and transactions from an address can form a bipartite graph after we link the review to the matched transaction. Portnoff matches specific ads to publicly available Bitcoin transactions based on the cost of ads and timestamp at which the ad was placed [38]. Hungarian algorithm and Hopcroft-Karp algorithm are two greedy algorithms that can successfully find the maximum matching in bipartite graph [39–41]. We can use these algorithms to find the maximum matching between a vendor and a Bitcoin address. However, this method is not effective enough to match multiple addresses. A vendor in the darknet normally owns a lot of Bitcoin addresses.

3.2.3 Submodular Function

Submodular optimization algorithm has been exploited in other areas before [42–45]. Kempe using a greedy algorithm based on submodular function to maximize the influence in

Table (3.1) Main Symbols

symbols	definitions
$b(t, u, r)$	a Bitcoin transaction with timestamp t, money value u, and receiving address r
B	a set of Bitcoin transactions, $B = \{b_i(t_i, u_i, r_i)\}$
R	a set of receiving Bitcoin addresses, $R = \{r_i\}$
$f(\tau, v)$	a feedback review with timestamp t and money value v
F	a set of feedback reviews, $F = \{f_j(\tau_j, v_j)\}$, from one vendor
θ, ϕ	bounding box thresholds of timestamp and money value
$S(R)$	a set function, input R: a set of receiving Bitcoin addresses, output: the set of feedback reviews matched with R
$s(R)$	a set function, input R: a set of receiving Bitcoin addresses, output: the number of feedback reviews matched with R, i.e., $s(R) = \lvert S(R) \rvert$, where $\lvert \cdot \rvert$ represents the cardinality of a set

social networks [46]. Leskovec exploits the submodularity of outbreak detection to develop an efficient approximation algorithm for water distribution and the blogosphere monitoring problem [47].

3.3 Problem Formulation

In this section, we formulate the problem of matching Bitcoin transactions with feedback reviews. Table 3.1 shows the main symbols used in this chapter and their definitions.

Let $B = (b_1(t_1, u_1, r_1), b_2(t_2, u_2, r_2), \cdots, b_n(t_n, u_n, r_n))$ represents the set of all Bitcoin transactions, where $b_i(t_i, u_i, r_i)$ represents a Bitcoin transaction with three attributes: timestamp t_i, money value u_i, and receiving address r_i. Here we only need receiver part of these Bitcoin transactions. Let R represent a set of all unique receiving addresses in B. Let $F = (f_1(\tau_1, v_1), f_2(\tau_2, v_2), \cdots, f_m(\tau_m, v_m))$ represents a list of feedback reviews received by one vendor, where $f_j(\tau_j, v_j)$ is a feedback review with two attributes: timestamp τ_j and money value v_j.

Vendor Receiving Address Set Problem:Finding a set of receiving addresses $R_k \subset R$ which are likely the Bitcoin addresses in the vendor's wallet, according to the matching between the vendor's feedback reviews in set F and Bitcoin transactions in set B.

Based on practical observations, the timestamp τ_j and money value v_j in $f_j(\tau_j, v_j)$

Table (3.2) An Example to Illustrate the Vendor Receiving Address Set Problem

Input	
all Bitcoin transactions B	feedback reviews F
$b_1(t_1, u_1, r_2)$	$f_1(\tau_1, v_1)$
$b_2(t_2, u_2, r_3)$	$f_2(\tau_2, v_2)$
$b_3(t_3, u_3, r_4)$	$f_3(\tau_3, v_3)$
$b_4(t_4, u_4, r_5)$	$f_4(\tau_4, v_4)$
$b_5(t_5, u_5, r_6)$	$f_5(\tau_5, v_5)$
$b_6(t_6, u_6, r_1)$	$f_6(\tau_6, v_6)$
$b_7(t_7, u_7, r_7)$	$f_7(\tau_7, v_7)$
$b_8(t_8, u_8, r_1)$	
$b_9(t_9, u_9, r_8)$	
$b_{10}(t_{10}, u_{10}, r_1)$	
$b_{11}(t_{11}, u_{11}, r_2)$	
$b_{12}(t_{12}, u_{12}, r_3)$	
$b_{13}(t_{13}, u_{13}, r_4)$	
$b_{14}(t_{14}, u_{14}, r_9)$	
$b_{15}(t_{15}, u_{15}, r_1)$	
$b_{16}(t_{16}, u_{16}, r_3)$	
$b_{17}(t_{17}, u_{17}, r_5)$	
$b_{18}(t_{18}, u_{18}, r_1)$	
$b_{19}(t_{19}, u_{19}, r_3)$	
$b_{20}(t_{20}, u_{20}, r_2)$	
$b_{21}(t_{21}, u_{21}, r_{10})$	
$\cdots$	

After matching		
feedback reviews F	Bitcoin transactions	receiving addresses
$f_1(\tau_1, v_1)$	$b_1(t_1, u_1, r_2)$	r_2
	$b_2(t_2, u_2, r_3)$	r_3
	$b_3(t_3, u_3, r_4)$	r_4
	$b_4(t_4, u_4, r_5)$	r_5
	$b_5(t_5, u_5, r_6)$	r_6
$f_2(\tau_2, v_2)$	$b_6(t_6, u_6, r_1)$	r_1
	$b_7(t_7, u_7, r_7)$	r_7
$f_3(\tau_3, v_3)$	$b_8(t_8, u_8, r_1)$	r_1
	$b_9(t_9, u_9, r_8)$	r_8
$f_4(\tau_4, v_4)$	$b_{10}(t_{10}, u_{10}, r_1)$	r_1
	$b_{11}(t_{11}, u_{11}, r_2)$	r_2
	$b_{12}(t_{12}, u_{12}, r_3)$	r_3
	$b_{13}(t_{13}, u_{13}, r_4)$	r_4
	$b_{14}(t_{14}, u_{14}, r_9)$	r_9
$f_5(\tau_5, v_5)$	$b_{15}(t_{15}, u_{15}, r_1)$	r_1
	$b_{16}(t_{16}, u_{16}, r_3)$	r_3
	$b_{17}(t_{17}, u_{17}, r_5)$	r_5
$f_6(\tau_6, v_6)$	$b_{18}(t_{18}, u_{18}, r_1)$	r_1
	$b_{19}(t_{19}, u_{19}, r_3)$	r_3
$f_7(\tau_7, v_7)$	$b_{20}(t_{20}, u_{20}, r_2)$	r_2
	$b_{21}(t_{21}, u_{21}, r_{10})$	r_{10}

are approximately equal to the timestamp t_i and money value u_i in a Bitcoin transaction $b_i(t_i, u_i, r_i)$ respectively, i.e., $\tau_j \approx t_i$ and $u_j \approx v_i$, if $b_i(t_i, u_i, r_i)$ is the corresponding Bitcoin transaction of the feedback review $f_j(\tau_j, v_j)$. By comparing the timestamp and money value attributes, we can match feedback reviews to Bitcoin transactions thus finding the receiving addresses. In case the vendor does not change the receiving addresses frequently, many of their feedback reviews will be matched with Bitcoin transactions with the same receiving addresses. Problem 3.3 aims at finding a set of receiving addresses $R_k \subset R$ whose involved Bitcoin transactions match the maximum number of feedback reviews in F.

We use a bounding box to find candidate Bitcoin transactions for a feedback review. For each review, we search the Bitcoin transactions B with a bounding box. We set thresholds θ and ϕ to constrict the ranges of timestamp and money value respectively. Currently, there

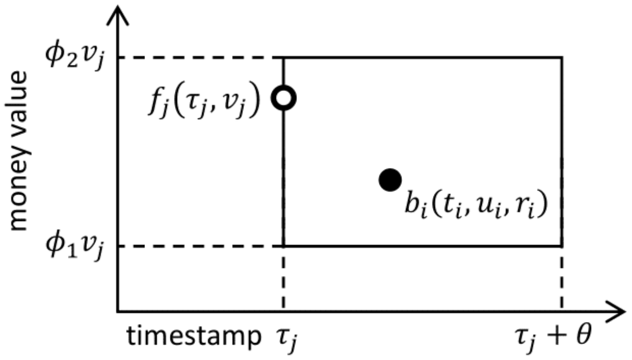

Figure (3.2) Bounding Boxes of Timestamp and Money Value for Matching a Feedback Review with a Bitcoin Transaction

are thousands of Bitcoin transactions every second. We compare a feedback review with a Bitcoin transaction and we are able to match a review to thousands of candidate transactions in real data with the range we provided. According to research [29], a Bitcoin transaction happens within an hour after a buyer posts the review with a high possibility. Therefore, we use $\tau_j \leq t_i \leq \tau_j + \theta$ as the bounding box for timestamp and set $\theta = 1$ hour. The market takes 5.5% commission fee and the exchange rate also fluctuates in a day. Therefore, we use $\phi_1 v_j \leq u_i \leq \phi_2 v_j$ as the bounding box for money value. If the fluctuation range is 10%, the setting will be $\phi_1 = (1 - 5.5\%)(1 - 10\%) = 0.8505$ and $\phi_2 = (1 - 5.5\%)(1 + 10\%) = 1.0395$. Figure 3.2 illustrates the bounding boxes. If a Bitcoin transaction $b_i(t_i, u_i, r_i)$ falls in the bounding boxes of a feedback review $f_j(\tau_j, v_j)$, we say b_i and f_j are a match, which is formally defined in Definition 3.3.

f_j **is matched with** b_i : A feedback review $f_j(\tau_j, v_j)$ is matched with a Bitcoin transaction $b_i(t_i, u_i, r_i)$ if $\tau_j \leq t_i \leq \tau_j + \theta$ and $\phi_1 v_j \leq u_i \leq \phi_2 v_j$.

Table 5.2 shows an example. The left part of Table 5.2 shows the input set B of Bitcoin transactions and the input set F of feedback reviews received by a vendor. Because of the limited space, only 21 Bitcoin transactions are shown here but B should contain hundreds of millions of transactions. In the example, the vendor has 7 feedback reviews. The right part of Table 5.2 shows the matches between the 7 feedback reviews and the 21 Bitcoin

Table (3.3) Vertical and Binary Format

receiving Bitcoin address r_i	feedback reviews $S(\{r_i\})$ matched with r_i	support $s(\{r_i\})$	binary format representation
r_1	f_2, f_3, f_4, f_5, f_6	5	0, 1, 1, 1, 1, 1, 0
r_2	f_1, f_4, f_7	3	1, 0, 0, 1, 0, 0, 1
r_3	f_1, f_4, f_5, f_6	4	1, 0, 0, 1, 1, 1, 0
r_4	f_1, f_4	2	1, 0, 0, 1, 0, 0, 0
r_5	f_1, f_5	1	1, 0, 0, 0, 1, 0, 0
r_6	f_1	1	1, 0, 0, 0, 0, 0, 0
r_7	f_2	1	0, 1, 0, 0, 0, 0, 0
r_8	f_3	1	0, 0, 1, 0, 0, 0, 0
r_9	f_4	1	0, 0, 0, 1, 0, 0, 0
r_{10}	f_7	1	0, 0, 0, 0, 0, 0, 1

transactions. To save space, we ignore the concrete values of timestamps and money values in B and F in the left part. Whenever there is a match, it means that the feedback review and Bitcoin transaction satisfy Definition 3.3. From the right part of 5.2, we can see that there could be multiple Bitcoin transactions that are matches of one feedback review. In real cases, a feedback review could match hundreds of Bitcoin transactions. And the receiving addresses in those matched Bitcoin transactions are the candidate addresses of the vendor.

In order to accelerate the computation in the later stages, we transfer the matching results to the vertical and binary formats in Table 3.3. To solve Problem 3.3, we aim at finding a minimum set of Bitcoin addresses covering all feedback reviews. The intuition is that a Bitcoin address that can cover many feedback reviews is very likely to belong to the vendor wallet. This is especially true when the careless vendor infrequently or barely changes their Bitcoin address.

Let $S(R)$ represents a set function which returns the set of feedback reviews that are matched with the input set R of Bitcoin addresses. Let $s(R)$ represent a set function which returns the number of feedback reviews matched with the input set R, i.e., $s(R) = |S(R)|$. Theorem 3.3 shows that $s(R)$ is a submodular set function [46].

Given three Bitcoin address sets A, B, C with $A \subseteq B \subseteq C$ and a Bitcoin address

$r \in C \setminus B$, we have

$$s(A \cup \{r\}) - s(A) \geq s(B \cup \{r\}) - s(B) \tag{3.1}$$

The left equation $s(A \cup \{r\}) - s(A)$ represents the number of feedback reviews that are newly matched after adding the Bitcoin address r to the set A. Thus, we have $s(A \cup \{r\}) - s(A) = s(\{r\}) - |S(A) \cap S(\{r\})|$. Similarly, $s(B \cup \{r\}) - s(B) = s(\{r\}) - |S(B) \cap S(\{r\})|$. Since $A \subseteq B$, A are matched with less or equal feedback reviews than B, i.e., $S(A) \subseteq S(B)$, we have $S(A) \cap S(\{r\}) \subseteq S(B) \cap S(\{r\})$ thus $|S(A) \cap S(\{r\})| \leq |S(B) \cap S(\{r\})|$. Therefore, $s(\{r\}) - |S(A) \cap S(\{r\})| \geq s(\{r\}) - |S(B) \cap S(\{r\})|$. This completes the proof.

Theorem 3.3 exhibits the diminishing returns property, which is the equivalent condition of a submodular set function. The property can be explained as that the marginal gain from adding a Bitcoin address to the set R is at least as high as the marginal gain from adding the Bitcoin address to a superset of R. We aim at finding a receiving address set R with size k, i.e., $|R| = k$, which can maximize $s(R)$.

We decompose Problem 3.3 into two steps, which are formulated as Problem 3.3 and Problem 3.3. Problem 3.3 aims at matching Bitcoin transactions with feedback reviews. Problem 3.3 aims at searching the optimal set of Bitcoin addresses for a vendor. The output of Problem 3.3 is the input of Problem 3.3.

Bounding Box Matching Problem: Given the set of Bitcoin transactions B, the set of feedback reviews F, and the bounding box parameters θ for timestamp, ϕ_1 and ϕ_2 for money values, the problem aims at finding a family of sets $\{S_i\}$, where S_i represents the set of feedback reviews covered by candidate receiving address r_i.

Maximum Review Coverage Problem: Given a family of sets $\{S_i\}$ with S_i representing the set of feedback reviews matched with each r_i in $b_i(t_i, u_i, r_i) \in B$ and a positive integer k as the budget for the number of receiving addresses, the problem is finding an address set R with size k, i.e., $|R| = k$, that are matched with the maximum number of feedback reviews. That is, finding the optimal solution R of the following optimization problem:

$$\begin{aligned} \max \quad & s(R) \\ \text{s.t.} \quad & |R| = k \end{aligned}$$

Problem 3.3 can be solved in polynomial time.

Problem 3.3 is NP-hard. Problem 3.3 can be reduced from the famous Set Cover problem [48]. Let $X = \{X_1, \cdots, X_q\}$ be a family of sets with $Y = \{y_1, \cdots, y_p\} = \bigcup_{i=1}^{q} X_i$ being the elements. The NP-complete Set Cover problem aims at finding whether there exist k of the subsets in $\{X_i\}$ whose union is equal to Y. Given an arbitrary instance of the Set Cover problem, we define a corresponding instance of Problem 3.3. For each subset $X_i \in X$, we create a Bitcoin address r_i and a set S_i. Therefore, we get a family of sets $\{S_i\}$ and $R_{\text{all}} = \{r_1, \cdots, r_q\}$, where all r_i's are unique. For each element y_j, we create a feedback review f_j. Therefore, we get $F = \{f_1, \cdots, f_p\}$. We add f_j to S_i, i.e., r_i is matched with f_j, if and only if X_i contains y_j. The Set Cover problem is equivalent to deciding if there is a set $R \subseteq R_{\text{all}}$ of k Bitcoin addresses with $s(R) = p$.

3.4 Computing Algorithms

In this section, we discuss how to efficiently compute the problems. We first study the bounding box and KD tree techniques for matching the Bitcoin transactions with feedback reviews. We then exploit a greedy algorithm that can obtain an address set that is provably cover $(1 - 1/e)$ ratio reviews of optimal. Here e is Euler's number. Finally, we propose our fast method which can accelerate the whole process by effectively reducing the times of matching.

3.4.1 Bounding Box and K-D tree

For each pair of feedback review $f \in F$ and Bitcoin transaction $b \in B$, we need to check the inequalities of timestamp and Bitcoin value. Let $n = |B|$ be the number of Bitcoin transactions in B and $m = |F|$ be the number of feedback reviews in F. It runs in $O(mn)$ to compare reviews with all Bitcoin transactions.

Algorithm 4: Build KD Tree(B, η, d) [49]

```
Input: Bitcoin transaction set $B$, max depth $\eta$, current depth $d$
Output: a KD-tree $T$
if $d < \eta$ then                                  // $d < \eta$, a non-leaf node of the KD-tree
    create a KD-tree $T$ with a root node $\pi$;
    if $d$ is odd then                               // $d$ is odd, split by the timestamp
        $\pi.t \leftarrow$ the median value of all timestamps in $B$;
        split $B$ into $B_1(t < \pi.t)$ and $B_2(t \geq \pi.t)$ by time;
    else                                             // $d$ is even, split by the money value
        $\pi.u \leftarrow$ the median value of all money values in $B$;
        split $B$ into $B_1(u < \pi.u)$ and $B_2(u \geq \pi.u)$ by value;
    $T_{\text{left}} \leftarrow \text{BuildKDTree}(B_1, \eta, d+1)$;       // build the left KD-tree
    $T_{\text{right}} \leftarrow \text{BuildKDTree}(B_2, \eta, d+1)$;      // build the right KD-tree
    add a left child sub-tree $T_{\text{left}}$ and a right child sub-tree $T_{\text{right}}$ to $\pi$;
else                                                 // $d = \eta$, a leaf node of the KD-tree
    create a KD-tree $T$ with a single node $\pi$ containing set $B$;
```

To speed up the search process, we build a 2-D tree for the Bitcoin transaction set B where the 2 dimensions are timestamp and money value. The reason that we build a KD-tree for B, not for F is that the number n of Bitcoin transactions is generally much larger than the number m of feedback reviews of a vendor. Algorithm 4 shows a recursive method for building a KD-tree with a fixed height η from set B. In the even depth nodes of the KD-tree, timestamp is used for partitioning the Bitcoin transactions. In the odd depth nodes of the KD-tree, money value is used. To build the entire KD-tree, we call "BuildKDTree(B, η, $d = 1$)" in algorithm 4 and pass the entire set B, the maximum depth η of the KD-tree, and the initial depth $d = 1$ to the function. Figure 3.3(a) shows an example of building a KD-tree and Figure 3.3(b) shows the resulting KD-tree. In each depth d, Algorithm 4 needs a linear time $O(n)$ to find the median and split the set into left and right subsets. Algorithm 4 runs in $O(\eta n)$.

Algorithm 5 shows the improved bounding box search algorithm using the KD-tree. For each feedback review f, Algorithm 5 will find the leaf nodes in the KD-tree that may contain Bitcoin transactions matched with f. Searching a KD tree runs in $O(2^\eta)$ in the worst case. W represents all leaf nodes of the KD-tree that are returned. In general, the number of returned leaf nodes is small. Suppose on average, the number of returned leaf nodes is

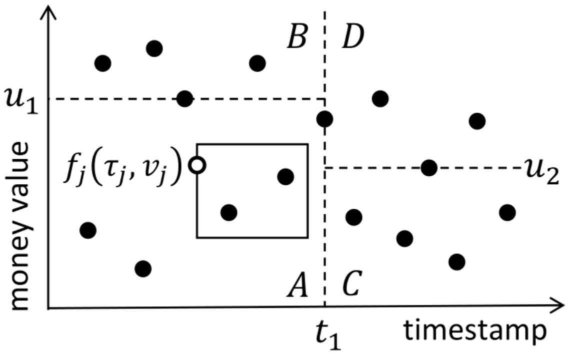

(a) coordinate system representation

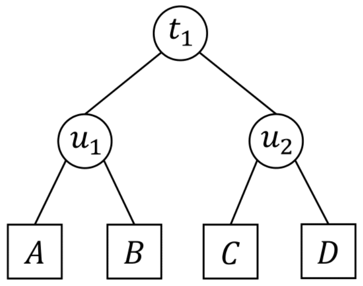

(b) tree representation

Figure (3.3) K-D Tree and Range Searching

Algorithm 5: Bounding Box Search with KD Tree(B, T, F, η, θ, ϕ_1, ϕ_2)

Input: Bitcoin transaction set B, KD-tree T built from B, feedback review set F, max depth η, bounding box parameter θ for timestamp, ϕ_1 and ϕ_2 for money value

Output: a family of sets $\{S_i\}$, where S_i represents the set of feedback reviews matched with r_i in $b_i(t_i, u_i, r_i) \in B$

```
for each unique $r_i$ in $b_i(t_i, u_i, r_i) \in B$ do $S_i \leftarrow \emptyset$;    // initialization
$f_j(\tau_j, v_j) \in F$ : $W$ = KDTreeSearch(root node of KD-tree $T$, $f(\tau, v)$, $\eta$, $\theta$, $\phi_1$, $\phi_2$);
$b_i(t_i, u_i, r_i) \in W$ : if $\tau_j \le t_i \le \tau_j + \theta$ and $\phi_1 v_j \le u_i \le \phi_2 v_j$ then
    $S_i \leftarrow S_i \cup \{f_j\}$;
```

γ. Since there are 2^η leaf nodes, there are $O(n/2^\eta)$ Bitcoin transactions in each leaf node. Therefore, Algorithm 5 runs in $O((\gamma + \eta)mn/2^\eta)$ on average. It is much faster than $O(mn)$. γ is small in our experiments on real data.

3.4.2 Greedy Set Cover Algorithm

Algorithm 6 shows a greedy algorithm with a ratio $(1 - 1/e)$ of optimal for solving Problem 3.3. In Algorithm 6, we start with an empty address set $R_0 = \emptyset$, and add a Bitcoin address r_i in each iteration which maximally increases the review coverage $s(R_i)$.

Algorithm 6 has an approximation ratio of $(1 - 1/e)$. That is, $s(R_k) \ge (1 - 1/e)s(A^*)$ where A^* represents the k-size address set which matches maximum reviews and k is the size of returned address set.

The proof can be found in [50]. The key observation is that $s(R)$ is non-decreasing submodular set function according to Theorem 3.3.

```
Algorithm 6: Greedy Set Cover Algorithm($\{S_i\}$, $\lambda$)
Input: a family of sets $\{S_i\}$, where $S_i$ represents the set of feedback reviews matched with $r_i$
       in $b_i(t_i, u_i, r_i) \in B$, a threshold $\lambda \in (0, 1)$
Output: optimal number $k$
$r_1 \leftarrow \text{argmax}_{r \in R}\, s(r)$; $R_1 \leftarrow \{r_1\}; i \leftarrow 1$;  // extract the best matching
$(s(R_i) - s(R_{i-1}))/(s(R_{i-1}) - s(R_{i-2})) < \lambda$  $r_{i+1} \leftarrow \text{argmax}_{r \in R \setminus R_i}(s(R_i \cup \{r\}) - s(R_i))$;
$R_{i+1} \leftarrow R_i \cup \{r_{i+1}\}$, $i++$;
return $R_{i-1}$;
```

```
Algorithm 7: Cost-Effective Addresses Searching($B$, $F$, $\theta$, $\phi_1$, $\phi_2$, $\lambda$)
Input: Bitcoin transaction set $B$, feedback review set $F$, bounding box parameter $\theta$ for
       timestamp, $\phi_1$ and $\phi_2$ for money value, a threshold $\lambda \in (0, 1)$
Output: a set $R_k$ of Bitcoin addresses belonging to a vendor
$R' \leftarrow \emptyset$; $F' \leftarrow \emptyset$; $\alpha' \leftarrow$ None;  // Stage 1: an address with max coverage
$s(\alpha') < |F \setminus F'|$  $F_{\alpha'} \leftarrow$ all feedback reviews matched with Bitcoin address $\alpha'$;
$f \leftarrow$ select a feedback review from $F \setminus (F' \cup F_{\alpha'})$ at random;
$R' \leftarrow R' \cup \{$ Bitcoin addresses matched with $f\}$; $F' \leftarrow F' \cup \{f\}$;
$\alpha' \leftarrow \text{argmax}_{r \in R'}\, s(r)$;      // extract the best matching address
$R_1 \leftarrow \{\alpha'\}$; $i \leftarrow 1$;           // Stage 2: searching for a set of addresses
$(s(R_i) - s(R_{i-1}))/(s(R_{i-1}) - s(R_{i-2})) > \lambda$  $F_{\alpha'} \leftarrow$ all feedback reviews matched with Bitcoin
address $\alpha'$;
$F \leftarrow F \setminus F_{\alpha'}; F' \leftarrow F' \setminus (F' \cap F_{\alpha'})$;
$\alpha' \leftarrow \text{argmax}_{r \in R'}\, s(r)$;  // best matching address based on new $F$
$R_{i+1} \leftarrow R_i \cup \{\alpha'\}$; $i++$;
return $R_{i-1}$;
```

Algorithm 6 can decide the number of addresses to return with a threshold λ. Intuitively a vendor's Bitcoin addresses should match many more of their feedback reviews compared with noise Bitcoin addresses that do not belong to them. This phenomenon is also proved in our experiments on real-life data. We calculate the ratio of increments in review coverage in two consecutive iterations. If the ratio is less than a threshold $\lambda \in (0, 1)$, the greedy algorithm will terminate and output address set.

3.4.3 Cost-Effective Addresses Searching

Algorithm 5 will find matched Bitcoin transactions for all feedback reviews in F. And the following greedy algorithm 6 will find an optimal address which cover most reviews iteratively. The whole process is time consuming. In this section, we propose a Cost-

Effective Addresses Searching(CEAS) algorithm which will find the optimal address with much less matching calculations between reviews and Bitcoin transactions. The steps are shown in algorithm 7. In CEAS, we only needs to apply range searching for $(|F|-s(r_{max})+1)$ reviews, where r_{max} is the address that covers maximum reviews. Therefore $s(r_{max})$ is the maximum number of reviews matched by a single address. Experiments show that CEAS can prunes about 60% comparisons between reviews and Bitcoin transactions.

Let F represents full feedback reviews and F' represents feedback reviews set which we have already applied range searching for. R is the address set containing all addresses and R' represents address set containing addresses matched by any reviews in F'. We have following theorem.

Let $\alpha = \text{argmax}_{r \in R}\, s(r)$ and $\alpha' = \text{argmax}_{r \in R'}\, s(r)$. If $s(\alpha') \geq |F \setminus F'|$, we have $\alpha' = \alpha$.

α is the address in R that matches the maximum number of reviews and α' is the address in R' that matches the maximum number of reviews. For any Bitcoin address $r \in R \setminus R'$, it doesn't match any reviews in F'. Therefore, the maximum number of reviews that r can match is $|F \setminus F'|$. If $s(\alpha')|F \setminus F'|$, address α' matches more reviews than any address $r \in$R $\setminus R'$, which makes α' the address that matches largest number of reviews in set R. This completes the proof.

According to Theorem 3.4.3, we can find the optimal address in R' which is also the optimal address we could find in R when the condition $s(\alpha') \geq |F \setminus F'|$ is satisfied. Therefore we don't need to apply range searching in KD-tree for all reviews in R to get this optimal address.

In all addresses R, to find the optimal address which matches maximum number of reviews in F, The number of feedback reviews $|F'|$ we need to apply range searching for is bounded as $|F| - s(r_{max}) \leq |F'| \leq |F| - s(r_{max}) + 1$.

r_{max} represents the address in R that matches maximum reviews. $s(r_{max})$ represents the number of feedback reviews that are matched with the address r_{max}. To satisfy the condition $s(\alpha')|F \setminus F'|$ in theorem 3.4.3, we have $|F'| \geq |F| - s(\alpha') \geq |F| - s(\alpha) = |F| - s(r_{max})$. At the same time, α need to match at least one review in F', which requires at most $(|F|-s(r_{max})+1)$

times of range searching.

Now we know we need at most $(|F| - s(r_{max}) + 1)$ times of range searching to get the optimal address. In greedy algorithm, we need to repeat this step for k times to obtain the optimal k-size address set. We can prove that finding the optimal address set still need at most $(|F| - s(r_{max}) + 1)$ times range searching.

To find optimal address set in greedy Algorithm 7, the total number of feedback reviews $|F'|$ we need to apply range searching is still bounded as $|F| - s(r_{max}) \leq |F'| \leq |F| - s(r_{max}) + 1$. After we apply $|F| - s(r_{max})$ or $|F| - s(r_{max}) + 1$ times of range searching to get the first address. The next address should be the one which matches maximum reviews in the remaining reviews based on greedy algorithm. We can remove reviews covered by the first address and use the same method to find the second address which matches maximum reviews in the remaining reviews. When we select feedback review to apply range searching in step 4 of algorithm 7, we avoid the reviews which are matched with address α'. As a result, in all $|F| - s(r_{max})$ feedback reviews where we apply range searching on, only one feedback review match with the address r_{max}. After we remove reviews covered by the address r_{max}. In the remaining $F - s(r_{max})$ reviews, there should be $|F| - s(r_{max}) - 1$ reviews that have already gone through range searching. Now we can update $F = (F - s(r_{max}))$ and update $F' = (|F| - s(r_{max}) - 1)$. Then the new $|F \setminus F'| = ((F - s(r_{max})) - (|F| - s(r_{max}) - 1) = 1$, which means $s(\alpha') \geq |F \setminus F'|$ in theorem 3.4.3 is always satisfied. Therefore we don't need to apply range searching to any more reviews to find remaining addresses of vendor.

Figure 3.4 explains CEAS Algorithm using the example in Table 5.2. In Figure 3.4, we use a bipartite graph to represent the matches between feedback reviews and receiver addresses. Each node on the left represents a feedback review and each node on the right represents a receiver address. An edge represents that a feedback review is covered by this address. A dotted edge represents a non-computed match and a solid edge represents a computed match. We re-order the nodes on both sides to reduce the visual clutter.

In Stage 1, Algorithm 7 randomly selects f_1 in line 4 and finds its matched Bitcoin addresses $\{r_2, r_3, r_4, r_5, r_6\}$ in line 5. Now $F' = \{f_1\}$ and $R' = \{r_2, r_3, r_4, r_5, r_6\}$. We use black

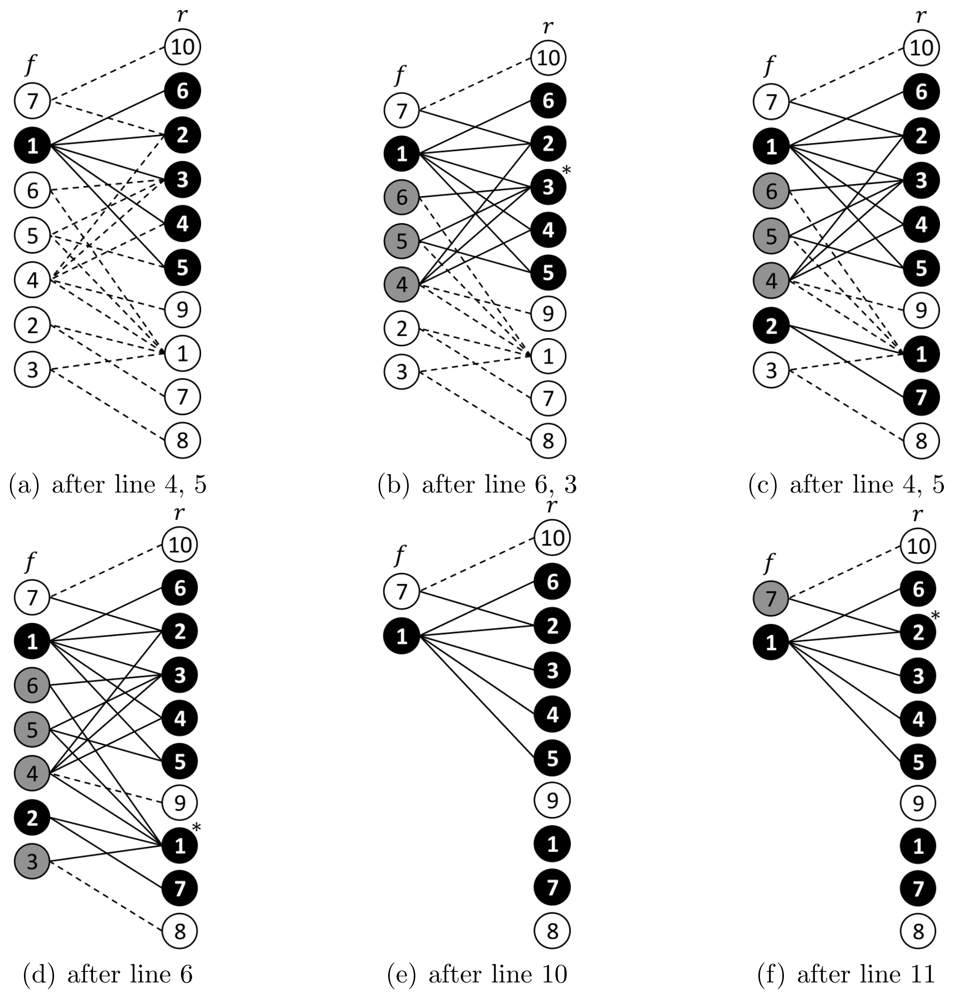

Figure (3.4) An Example for the Heuristic Search in Algorithm 7 (F: nodes on the left; F': black nodes on the left; R': black nodes on the right; the "line" refers to the lines in Algorithm 7)

nodes to represent them in Figure 3.4(a). Algorithm 7 extracts the Bitcoin address r_3 from R' since it has the largest number of matched feedback reviews. In Figure 3.4(b), we use "$*$" to represent the Bitcoin address in R' with the maximum coverage. Now $F_{\alpha'} = \{f_1, f_4, f_5, f_6\}$. Algorithm 7 then randomly selects f_2 from the review set $F \setminus (F' \cup F_{\alpha'}) = \{f_2, f_3, f_7\}$ in line 4 and finds its matched Bitcoin addresses $\{r_1, r_7\}$ in line 5. Now $R'= \{r_1, r_2, r_3, r_4, r_5, r_6, r_7\}$ and $F' = \{f_1, f_2\}$. Figure 3.4(c) shows the status. Algorithm 7 extracts the Bitcoin address r_1 from R' since it has the largest number of matched feedback reviews, which is shown in Figure 3.4(d). Since $s(r_{max}) = s(\{r_1\}) = 5 \geq |F \setminus F'| = 5$, Stage 1 is done.

In Stage 2, Algorithm 7 first adds the best Bitcoin address r_1 into the resulting set thus $r_{max} = r_1$. Since r_1 is matched with $F_{r_1} = \{f_2, f_3, f_4, f_5, f_6\}$, Algorithm 7 deletes the reviews covered by r_1 from the left part and the associated edges. Figure 3.4(e) shows the remaining graph. Now $F = \{f_1, f_7\}$ and $F' = \{f_1\}$. Algorithm 7 then selects the best matching address from R' based on the new $F = \{f_1, f_7\}$. Since r_2 has the largest number of matches thus is optimal. Algorithm 7 will terminate in the next iteration since all feedback reviews have been covered and the drop is larger than λ.

Here we only need to search matched Bitcoin transactions for f_1 and f_2. This is one possible solution for this example. In algorithm 7, we randomly select review to apply range searching. No matter how we select reviews, it always needs to apply range searching for 2 or 3 reviews in this example, which is the range of $|F'|$. In this example,$2 \leq |F'| \leq 3$ because $s(r_{max}) = 5$ and $|F| = 7$. In contrast, Algorithm 5 need apply range searching for all 7 feedback reviews. According to Theorem 3.4.3, Algorithm 7 always finds the same best Bitcoin address that Algorithm 6 finds.

Time Complexity: Line 5 in Algorithm 7 performs the bounding box search and is the most time consuming step and dominates the time complexity. This is because the number of Bitcoin transactions n is much larger than other parameters like m. Based on Theorem 3.4.3, the times of running line 5 is upper bounded by $|F'| \leq m - s(r_{max}) + 1$. Thus Algorithm 7 runs in $O((\gamma + \eta)(m - s(r_{max}) + 1)n/2^{\eta})$. Please refer to last paragraph in Section 3.4.1 for more details.

3.5 Experimental Results

In this section, we conduct extensive experiments to evaluate the efficiency and effectiveness of our method by using both real and synthetic datasets. All algorithms are implemented in Python and all the experiments are conducted on a Linux Server with Intel Xeon 3.2GHz CPU and 32 GB main memory.

Datasets. For the real dataset, we crawled feedback from Wall Street Market. Wall Street Market sells a variety of content, including drugs, stolen data, and counterfeit consumer goods, all using cryptocurrency. In the Wall Street market, each vendor has a list of reviews. Each feedback contains the time when the buyer leaves this feedback as well as the amount of Bitcoin used in this transaction. Here we crawled the feedback of different vendors and sum the transactions to a file, one transaction was represented by a 2-dimensional data (τ, v), where τ is the timestamp when this review was posted and v is money cost in this purchase. Here, we collect transactions of different vendors in Dec 2018. There are in total 17,155,754 Bitcoin transactions during this time. The synthetic dataset is produced by the Bitcoin transaction data.

Next, we first evaluate the efficiency of K-D tree and greedy algorithm by real dataset and then the accuracy by synthetic dataset.

3.5.1 Efficiency Evaluation in Range Searching

Each review we have can generate a 2-dimensional range based on the Bitcoin value and timestamp. With this range, we search the Bitcoin public ledger to find a lot of candidate transactions matched to this review. Figure 3.5 demonstrates that the K-D tree we build can effectively save time during range searching. We build a K-D tree with the real dataset, separating transactions into 16,384 buckets with a 14-depth binary tree. Each bucket contains more than one thousand transactions. We sample reviews from Wall Street Market. Bitcoin transactions are divided through Bitcoin value and timestamp alternately. Figure 3.5(a) shows the comparison of time-consuming in K-D tree and traversal in full ledger. It only takes less than 5.5 seconds to find the matched transactions for 1000 reviews in the K-D tree, nearly 5.5 milliseconds for one review. We also built another K-D Tree with a smaller data size, including only mixed transactions in Bitcoin public ledger. Users in cryptomarkets prefer mixed transactions to protect their privacy in Bitcoin transactions. We conduct the same experiment in this filter ledger which contains 1,395,694 Bitcoin transactions. Figure 3.5(b) shows the result with K-D tree structure; it only takes around 2 milliseconds to find the matched transactions for a review.

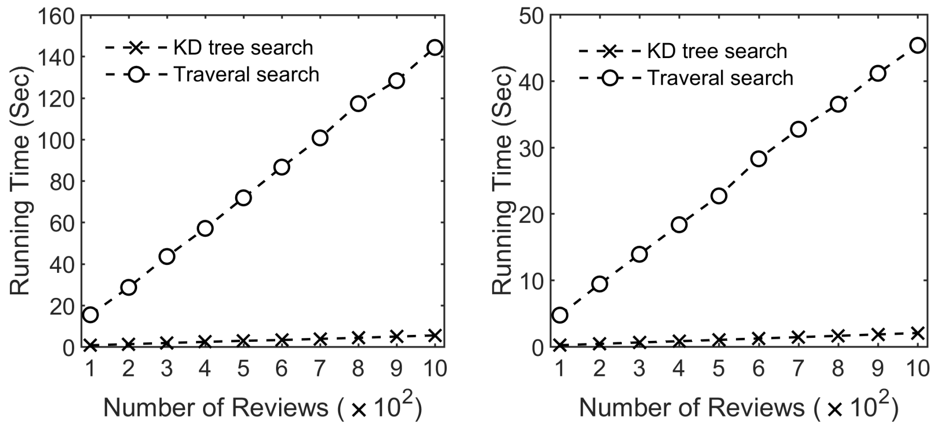

(a) range searching in full ledger (b) range searching in filtered ledger

Figure (3.5) Compare Running Time of K-D Tree Searching and Traversal Searching in Full Ledger and Filter

3.5.2 Effectiveness Evaluation of Greedy Algorithm

Our greedy algorithm guarantees that we can achieve at least $(1 - 1/e)$ of maximum coverage theoretically. Here we speed up our greedy algorithm by removing low degree addresses found in range searching and evaluate the performance of the greedy algorithm on the real dataset.

We select feedback from 100 vendors with 3721 reviews. Matched Bitcoin transactions of reviews from a vendor can be found through the K-D tree, which helps us get matched addresses of each review. By changing this data format to vertical format like Table 3.3, we get the reviews covered by each matched address for a vendor. Now we are looking for a receiver address set whose transactions can match the maximum reviews. Based on the range we set, a review can normally be matched to thousands of transactions in the Bitcoin ledger. Only one of these matched addresses can be the vendor's address, which means the remaining addresses are noises in our algorithm. In the experiments, 94.23% of the addresses we found only match one review. 5.26% of addresses match 2 reviews and only 0.51% addresses match more than 2 reviews on average. Heuristically we are looking for addresses that can match the maximum reviews. Therefore, removing addresses with a low degree will not affect the accuracy of our algorithm. We conduct the simple greedy

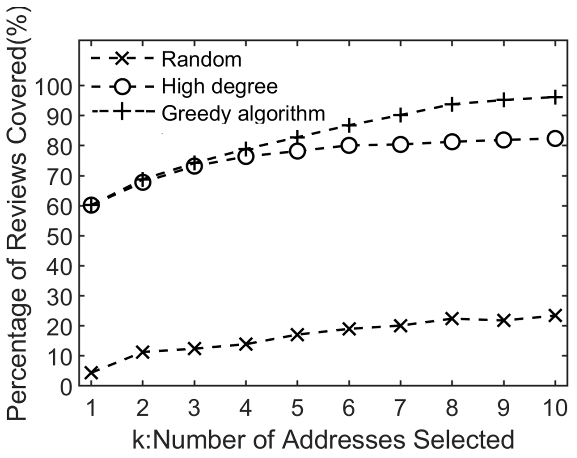

Figure (3.6) Greedy Agorithm Outperform High Degree and Random Method

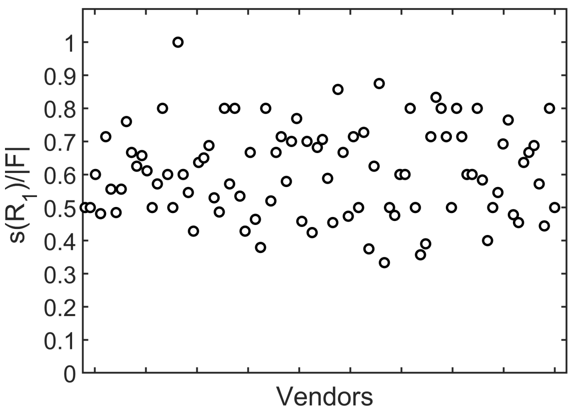

Figure (3.7) Maximum Reviews Covered by One Address in Ratio for Different Vendors

algorithm without setting a threshold λ. We set k from 1 to 10 as the number of output addresses. The greedy algorithm needs to output an address set that covers as many reviews as possible. Result demonstrates that we can save 93% time if we ignore address matching with only 1 review during the greedy algorithm and 99% time if we remove addresses with a degree less than 3.

To evaluate the performance in the maximum coverage of the greedy algorithm. We compare the greedy algorithm with a heuristic high degree method and the random selection method. The high degree method will select addresses with the maximum review coverage.

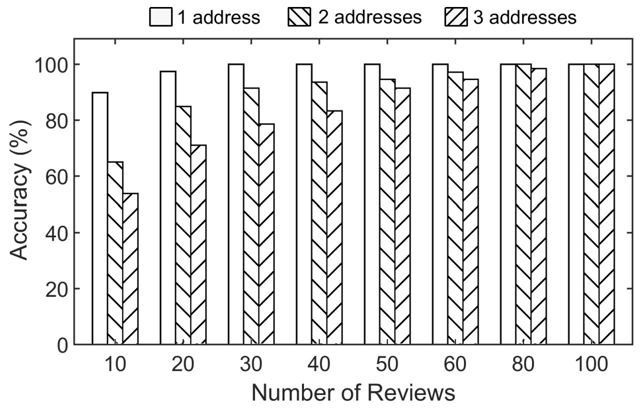

Figure (3.8) Accuracy Comparison Between Vendors with Different Number of Addresses

We average the percentages of reviews covered. From Figure 3.6, we can notice that the performance of the high degree method is similar to the greedy algorithm when k is small. As k increases, the gap between these two methods increases.

The number of times in range searching is at most $|F| - s(R_1) + 1$ in our proposed algorithm. We can reduce at least $s(R_1) - 1$ times. $s(R_1)$ is the number of reviews covered by the first address we get in the greedy algorithm, which also is the address r_{max} that covers maximum reviews in F. The more reviews covered by this address, the fewer times of range searching are required. Figure 3.7 shows the ratio $s(R_1)/F$ of 100 vendors we find in Wall Street Market. Each node in Figure 3.7 represents a vendor. We can see that the address which covers the maximum reviews can cover between 35% to 90% of all reviews from a vendor and 60.217% on average, which means we can reduce times of range searching by 60.217%. We find 66% of these vendors whose reviews can be matched to an address that covers more than half of the reviews. The result shows the effectiveness of our algorithm in the real dataset and unveils that the vendors in Wall Street Market do not change their receiving addresses frequently.

3.5.3 Accuracy Evaluation on Synthetic Data

In this section, we conduct experiments to evaluate the accuracy of our algorithm on synthetic reviews. We select 2000 Bitcoin addresses and collect their history transactions. Each transaction contains timestamp and Bitcoin value received, which can be treated as a review after a slight change. We apply normal distribution on the amount of change in both Bitcoin value and timestamp. The number of hours we advance on timestamp follows the normal distribution with 0.5 mean and 0.6 std. In probability, the newly generated review's bounding box in timestamp will cover the transaction at 59% feasibility. The same strategy is applied to the Bitcoin value. After combining the restrict of timestamp and Bitcoin value, the newly generated review can match to the original transaction with a 35.4% possibility. Every address we randomly select from the Bitcoin ledger can generate a synthetic review list. Considering vendors may use multiple Bitcoin addresses, we also combine some synthetic reviews generated by different addresses.

Figure 3.8 shows the accuracy of the greedy algorithm with reviews generated by 1 address, 2 addresses, and 3 addresses. Accuracy is the number of correct addresses over the number of addresses that generate these synthetic reviews. From Figure 3.8, we can see that longer review lists contribute to better accuracy, while more receiver addresses can reduce accuracy, which matches the real situation. It is hard to find the vendor's address set if the vendor updates their receiver address in the darknet market very frequently. For vendors who do not change their receiver address frequently, our algorithm can achieve great performance even with very few reviews.

We set a threshold λ for the ratio of new reviews covered in the current step to new reviews covered in the last step. We use synthetic data generated by different numbers of addresses to evaluate the effect of different λ. For reviews generated from one address, Figure 3.9 shows larger λ has better performance because we do not want to select another address besides the one with the highest degree. Reviews derived from 2 or more addresses share a similar pattern. Large λ can decrease the accuracy because a high threshold will stop the greedy algorithm too early and output fewer addresses than the vendor have. The more

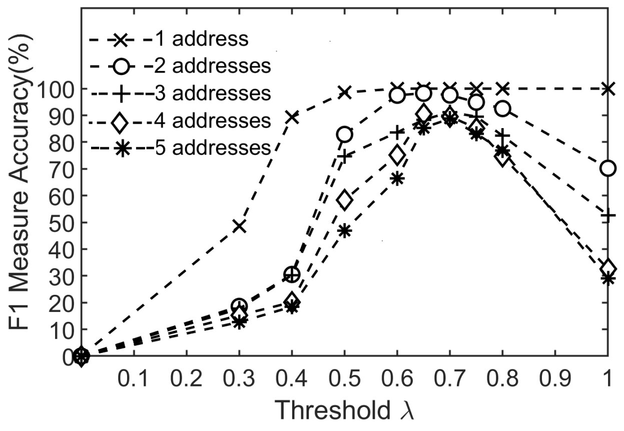

Figure (3.9) F1 Measure Accuracy of Synthetic Data Generated from Different Number of Addresses

addresses a feedback related, the fast the drop of accuracy after λ pass 0.7. Through the experiments, we can see λ around 0.7 is the best option for all these data.

3.6 Conclusion

In this chapter, we study the problem of identifying the Bitcoin addresses of a vendor by matching their feedback reviews with Bitcoin transactions. We firstly construct a K-D tree to efficiently match Bitcoin transactions to feedback reviews. After we obtain the matching relationship between Bitcoin transactions and feedback reviews, we get the address set by applying a greedy algorithm that can achieve a near-optimal theoretical guarantee. We further develop a Cost-Effective Address Searching(CEAS) algorithm that can speed up the process by pruning the search space effectively. Comprehensive experiments on both real and synthetic datasets demonstrate the effectiveness and efficiency of our methods.

PART 4

LEARNING INFECTIVITY GRAPH IN CHAT GROUP VIA TEMPORAL-TEXTUAL MULTI-DIMENSIONAL HAWKES PROCESS

In this chapter, we propose an effective model to discover hidden infectivity networks between members in a group chat.

4.1 Motivation

Telegram, as one of the most popular instant message applications, becomes the base for criminal activities. For example, the "Nth Room" case. The "Nth Room" case is a criminal case involving blackmail, cybersex trafficking, and the spread of sexually exploitative videos via the Telegram app between 2018 and 2020 in South Korea. The channel "Nth Room" in Telegram is where criminals communicate and commit activities. Telegram also has many public chat channels with illegal content. We can search the name of darknet market in Telegram. All these darknet markets manage a public chat channel in Telegram and we can easily find these chat channels and join them. Learning Granger causality for members in a chat group is meaningful for law enforcement. The Granger causality among members helps us to construct an influence network, which is beneficial to discover organizations behind these criminal activities and the related key person.

Unfortunately, identifying influence between members in a public group chat is not a simple task when there are thousands of members. Analyzing from a large amount of chat conversations could be challenging and time-consuming. Existing works about group chat mainly focus on community detection or topic detection. Farkhund applies data mining and natural language processing techniques on chat log[51, 52]. They proposed a framework which extracts the social network from chat logs and summarizes conversation into topics. Anwar presents a unified social graph based text mining framework to identify digital evidences from chat logs data[53], which considers both users' conversation and interaction data in group chats to discover overlapping users' interests and their social ties. However, these researches didn't investigate directional impact between members.

4.2 Related Work

We perform a literature review focusing on following two aspects: 1) Problems about multiparticipant chat analysis and how these have been addressed. 2) Hawkes processes for their dominant usages in self- exciting or mutual-exciting event sequence learning subsectionMultiparticipant Chat Communications through instant message applications have remained under a substantial study over the last few years. Due to increasing popularity, both structural and textual content of chat data are being investigated in various perspectives. Researchers have mainly focused on problems including preprocessing of text data[54–56], conversations disentanglement [57–60], topic detection[51, 52, 61] and community detection in chat logs[51–53, 62, 63].

There is a lot of overlap between chat preprocessing techniques and those used in other forms of microtext— normalizing the unusual, informal text characteristics. Each has described an expanded taxonomy of semiotic classes for text[54]. Sproat and Jaitly present a recurrent neural net (RNN) model of text normalization[56], where they model text normalization as a sequence-to-sequence problem. Chua et al. describes an automated multi-language text normalization infrastructure that prepares textual data to train language models used in Google's keyboards and speech recognition systems, across hundreds of language varieties[55].

A common phenomenon in group chats is that multiple conversations are mixed together. In group chat, a newly sent message may not be the response of the latest message when multiple conversations occur simultaneously. Therefore thread disentanglement is one of the major task in group chat analysis. In [57], Elsner proposes a graph-theoretic model for disentanglement, using discourse-based features which have not been previously applied to thread disentanglement. Focusing on NLP techniques on real dataset, Kauttonen analyzed two conversational corpora: A public library question-answering (QA) data and a private medical chat data they developed response retrieval (ranking) models using TF-IDF, StarSpace, ESIM and BERT methods [60]. For researchers who want to learn their thread disentanglement models with annotated datasets, Kummerfeld et al. released a new dataset of 77,563 messages manually annotated with reply-structure graphs that both disentangle conversations and define internal conversation structure[58].

Topic detection and community detection is high level analysis in group chat analysis. Many efforts have been made to extract key topics and network from large chat logs. In [51, 52], Iqbal first discovers the communities based on the co-occurrence frequencies of the entities in chat sessions, further they mine corresponding concepts by identifying important terms based on their frequency in the text. Anwar presents a unified social graph based text mining framework to identify digital evidence from chat logs data[53]. To study the characteristics of chat messages, Dong et al. analyzes a collection of 33,121 sample messages gathered from 1,700 sessions of conversations and concludes indicative term-based approach is superior to the traditional document frequency based approach, for feature selection in chat topic categorization[61]. In this chapter, we work with Hawkes process model to extract mutual influence factors, instead of detecting communities directly.

4.2.1 Hawkes Process

Hawkes processes [64] have been widely used to model time-series events where the occurrences of previous events could trigger the occurrences of future events. Those models successfully discover the influence network among events and predict future time-dependent event sequences. Researchers link triggering kernels of Hawkes process to granger causality of different event types successfully[65–70]. It has been utilized in areas including earthquake shocks prediction[71, 72], financial markets analysis [73, 74], health analysis[69, 75] and criminal activities[70, 74].

Several teams have achieved remarkable results in Hawkes process for mutual-exciting event sequence learning. Zhou et al. focuses on the nonparametric learning of the triggering kernels in Hawkes process[67], proposing an approach to discover the hidden network of social influence in sparse low-rank networks[66]. Linderman develops a probabilistic model that combines Hawkes processes with random graph models and discovers the latent network of stock trading, gangs activities and calcium imaging[74, 76]. Through an infinite order autoregression, Eichler designs a new nonparameteric estimator of the impact functions of the Hawkes process[65]. They apply this model to neural spike train data and study the mutual-exciting networks of spinal dorsal horn neurons under different conditions. Xu et al. represents the kernel functions with a series of basis functions and extract the influence graph through group sparsity of the kernel functions' coefficients.[68].

Howkes process can also be modeled to predict time series data. Xu et al. develops a novel framework based on Hawkes process to predict patient flow[69]. His team further model incomplete sequence data with Hawkes process by leveraging the idea of data synthesis[77]. They also discuss an effective model-based clustering method based on a novel Dirichlet mixture model of Hawkes process[78].

Most of the kernel functions of Hawkes process in existing works are decaying functions like power-law functions or exponential functions based on time. In this chapter we embed the text information from group chat into the kernel function of Hawkes process to describe a more precise influence network.

4.3 Proposed Model

As time series data, the chat history of a group can be considered as event sequence set $C = \{S^1, S^2, ...\}$, where sequence S^k represents a segment of chat in a chat group. Every $S^k = ({m_1}^k, {m_2}^k, ...)$ is a sequence of message ${m_i}^k = ({t_i}^k, {d_i}^k, {x_i}^k)$ where ${t_i}^k$ is time when the message was sent, ${d_i}^k$ is the member identity who sent this message and ${x_i}^k$ is the text content.

To uncover the latent infectivity network in group chat, our method contains two steps. **dialogue Classifier**: For a message m_j in group chat, to find which message it replied to, we embed each pair of messages (m_i, m_j) to a number $e_{ij} \in \{0, 1\}$ based on semantics in

text from m_i and m_j. Here e_{ij} classify whether that message m_j replies to m_i semantically.
Text biased Marked Multi-dimensional Hawkes Process: We model the chat history with a multi-dimensional hawkes process. In this model, message sequences in chat history are event sequences and the sender of the message is marked as the type of this event. We train this model based on observed chat history with learned dialogue classifiers.

4.3.1 Dialogue Classifier

In group chat, we want to get the relationship between the current message and previous messages semantically. They could be irrelevant or the current message is the response to one or several previous messages.

In this chapter, we pretrain text pairs with a BERT model, followed by a classifier. BERT is designed to pretrain deep bidirectional representations from text by jointly conditioning on both left and right context in all layers[79]. It's empirically powerful and has obtained state-of-art results on several natural language processing tasks. We input two texts to Bert pretained model which converts text pairs to a vector. This vector is further input to a downstream task classifier to fine-tune the pretrained Bert model. The classifier will classify whether the second text is a reply to the first text or not semantically. The output of the last layer should be a number $e \in \{0, 1\}$. Here $e = 0$ means it is not a reply and $e = 1$ represents it is. We can use this output number as the measure of the second text replying to the first text.

For message m_i, the message it replies to should be close with message m_i in time. In group chat, members normally wouldn't reply to a message a long time ago. Therefore, it's not necessary to calculate reply embedding of each pair of messages and only consider message pairs Within a limited time frame.

4.3.2 Temporal-Textual Multi-dimensional Hawkes Process

Although hawkes process can model time series sequence, there are two limitations of the one-dimensional hawkes process for our problem. One is that it can only model a single type of event. If we want to capture the interacting processes between members in a chat group, message sequences from different members should be treated as different types of events. Another limitation is that triggering the kernel only decays with time difference. Reply embedding of message pairs can also help us quantify the influence of a past event on the new event. If two messages are not classified as a conversation, we are supposed to know the previous message will not trigger the later message. Therefore we need a multi-dimensional hawkes process including reply embedding.

In our problems, message sequences in chat history are event sequences that we try to model. Sender d of the message could be marked as the type of this message. Multi-dimensional hawkes process can capture the mutual excitations among different types of events. Instead of using α to represent influence strength from previous events, we have matrix $A = [\alpha_{ij}]$ capturing the mutual influence in a group. Given event sequences $((t_1, d_1), (t_2, d_2), ...)$, the intensity function of type d at time t is

$$\lambda_d(t) = \mu_d + \sum_{j:t_j<t} \alpha_{d_j d} \cdot g(t - t_j) \tag{4.1}$$

where μ_d is exogenous base intensity of event type d. Here it means base activity level of user d in this group chat. The second term on the right side are influence from previous messages. $\alpha_{d_j d}$ is the strength of influence from person d_j on person d in this group.

If the new message is not a reply to a previous message, this new message is not triggered by this previous message. To leverage text information between current message $m_i(t_i, d_i, x_i)$ and a previous message $m_j(t_j, d_j, x_j)$, we update trigger kernel from $g(t_i - t_j)$ to $g(t_i - t_j) \cdot h(x_j, x_i)$, where $h(x_j, x_i) \in \{0, 1\}$ is the reply embedding. Give chat history $((t_1, d_1, x_1), (t_2, d_2, x_2), ...)$, the intensity function of member d at time t with text x is

$$\lambda_d(t, x) = \mu_d + \sum_{j:t_j<t} \alpha_{d_j d} \cdot g(t - t_j) \cdot h(x_j, x) \tag{4.2}$$

Here we utilize the reply embedding $h(x_j, x)$ to filter the influence from previous messages. Only messages responded by a new message have influence on the occurrence of this new message.

4.3.3 Learning Task

To find the infectivity matrix $A = [\alpha_{ij}]$, we need to derive the likelihood function of this hawkes model. Suppose we have a chat history $H = ((t_1, d_1, x_1), (t_2, d_2, x_2), ...(t_n, d_n, x_n))$, Let $F(t|H)$ be the conditional probability that next message $(t_{n+1}, d_{n+1}, x_{n+1})$ appears before time t, where $t > t_n$. We have $F(t|H) = P(t_{n+1} < t)$. And let $p(t|H)$ be the corresponding conditional probability density function. Then we have expected instantaneous happening rate of message $\lambda(t) = p(t|H)/(1-F(t|H))$, from where we can get the conditional probability density function for a specific member d with text x as

$$p_d(t, x|H) = \lambda_d(t, x) \cdot e^{-\int_{t_n}^{t} \lambda(\tau)d\tau} \tag{4.3}$$

Here $e^{-\int_{t_n}^{t} \lambda(\tau)d\tau}$ is the probability that the next message appears after time t based on given history H. $\lambda_d(t, x)$ is the intensity function of user d at time t sending text x.

Let event sequence $S = \{(t_i, d_i, x_i)\}_{i=1}^{N}$ represents chat history we observed in $t \in [0, T]$, we can derive the likelihood function of observed sequence as:

$$\prod_{i=1}^{N} p_{d_i}(t_i, x_i|H_i) e^{-\int_{t_N}^{T} \lambda(\tau)d\tau} \tag{4.4}$$

where H_i is the history events before time t_i.

Put intensity function into equation(4), the log-likelihood can be expressed as:

$$L(A) = \sum_{i=1}^{N} log \left(\mu_{d_i} + \sum_{j=0}^{i-1} \alpha_{d_j d_i} \cdot \beta e^{-\beta(t_i - t_j)} \cdot h(x_j, x_i) \right)$$

$$- \left(\sum_{d} \mu_d \cdot T + \sum_{d} \sum_{j=1}^{N} \alpha_{d_j d}(1 - e^{-\beta(T - t_j)}) \right) \tag{4.5}$$

The learning problem is to find the matrix $A = [\alpha_{ji}]$ that maximizes log-likelihood function $L(A)$.

4.3.4 EM Algorithm

We need to find Matrix $A = [a_{ij}]$ that maximizes log-likelihood function $L(A)$. From research [80], $L(A)$ is concave. We can apply EM algorithm to solve this optimization problem iteratively. In particular, we construct a tight lower-bound likelihood function for current parameter estimation by Jensen's inequality:

$$L(A) \geq \sum_{i=1}^{N} \left(\sum_{j=1}^{i-1} p_{ji} log \frac{\alpha_{d_j d_i} \cdot \beta e^{-\beta(t_i - t_j)} \cdot h(x_j, x_i)}{p_{ji}} + \ p_{ii} log \frac{\mu_{d_i}}{p_{ii}} \right.$$

$$\left. - \left(\sum_{d} \mu_d \cdot T + \sum_{d} \sum_{j=1}^{N} \alpha_{d_j d} (1 - e^{-\beta(T - t_j)}) \right) \right) \tag{4.6}$$

Here p_{ii} represents the probability that i^{th} event occurred due to base intensity μ_{d_i}. And p_{ji} can be interpreted as the probability that the i^{th} event is triggered by the j^{th} event. We have $\sum_{j=1}^{j=i} p_{ji} = 1$.

We can maximize our log likelihood by maximizing this lower bound. The EM algorithm for the estimation of the parameters is as follows. Starting with a guess $A = [\alpha_{ji}]$ for the parameters, iterate the following until convergence is reached:

Expectation-step:

$$p_{ii}^{(m)} = \frac{\mu_{d_i}^{(m)}}{\mu_{d_i}^{(m)} + \sum_{j=0}^{i-1} (\alpha_{d_j d_i}^{(m)} \cdot \beta e^{-\beta(t_i - t_j)} \cdot h(x_j, x_i))} \tag{4.7}$$

$$p_{ji}^{(m)} = \frac{\alpha_{d_j d_i}^{(m)} \cdot \beta e^{-\beta(t_i - t_j)} \cdot h(x_j, x_i)}{\mu_{d_i}^{(m)} + \sum_{j=0}^{i-1} (\alpha_{d_j d_i}^{(m)} \cdot \beta e^{-\beta(t_i - t_j)} \cdot h(x_j, x_i))} \tag{4.8}$$

Maximization-step:

$$\mu_u^{(m+1)} = \frac{\sum_{i=1, d_i = u}^{N} p_{ii}^{(m)}}{T} \tag{4.9}$$

$$\alpha_{uv}^{(m+1)} = \frac{\sum_{i=1,d_i=v}^{N} \sum_{j=1,d_j=u}^{i-1} p_{ji}^{(m)}}{\sum_{j=1,d_j=u}^{N} (1 - e^{-\beta(T-t_j)})} \tag{4.10}$$

Here u, v can represent any uses in group chat. It's guaranteed that EM algorithm is able to converge to the global maximum. We won't show details here.

4.4 Experiments

In this section, we first compare the performance of bert-based language model with XLNet-based language model in classification. we then conduct experiments using synthetic group chat generated from different sources of dialogue and real world group chat from telegram to fully evaluate the performance of our developed temporal-textual multi-dimensional Hawkes model in infectivity Graph learning.

4.4.1 Dialogue Classifier Comparisons

Bert, as the state of art language representation model, is designed to pre-train deep bidirectional representations from text by jointly conditioning on both left and right context in all layers[79]. Before the emergence of Bert, existing approaches like ELMo and OpenAI GPT use unidirectional language models to learn general language representations. Bert alleviates the unidirectionality constraint by using a "masked language model" (MLM) pre-training objective. Besides Bert, another state of art language representation model XLNet also has the capability of modeling bidirectional contexts [81].

Here we compare the performance of the Bert-based model with the XLNet-based model with the same size parameters. We train and test accuracy of the dialogue classifier based on data we crawled from telegram group channels. In telegram, users are able to click the reply button to reply to a specific utterance in group chat. Therefore a small part of utterance in group chat explicitly shows which utterance it replies to and we are able to parse these dialogue pairs of sentences. We can also select two random texts from group chat to create a non-dialogue sentence pair.

Dialogue Datasets Besides chat logs from telegram, we train and test the performance of dialogue classifiers with some public chitchat data as well. Here are the dialogue dataset we used to train and evaluate our models.

- **BSTalk** BlendedSkillTalk is a dataset of 7k conversations explicitly designed to exhibit multiple conversation modes: displaying personality, having empathy, and demonstrating knowledge [82].
- **ConvAI** A dataset of Human-bot dialogues containing free discussions of randomly chosen paragraphs from SQuAD.
- **CMUDoG** CMU Document Grounded Conversations is a document grounded dataset for text conversations, where the documents are Wikipedia articles about popular movies. Consists of 4112 conversations with an average of 21.43 turns per conversation[83].
- **DSTC7** DSTC7 provides a dataset of dialogs that are derived from collections of two-party conversations. The conversations are randomly split part way through to create a partial conversation and the true follow-up response.[84].
- **PersonaChat(PC)** A chit-chat dataset where paired Turkers are given assigned personas and chat to try to get to know each other response.[85].

Table4.1 shows the data size of training data, which is the number of sentences pairs. Table5.1 shows the classifier accuracy in different datasets. We can see the bert-based language model outperform the XLNet-based model in all of these datasets.

Table (4.1) Data Size

Training Data	Telegram	BSTalk	ConvAI	CMUDoG	DSTC7	PC
Size	33368	104898	5602	38082	27882	48547

Table (4.2) Accuracy of Dialogue Classifiers

Model	Telegram	BSTalk	ConvAI	CMUDoG	DSTC7	PC
Bert-based	**0.8044**	**0.9343**	**0.7068**	**0.7732**	**0.7881**	**0.8452**
XLNet-based	0.7154	0.8692	0.5524	0.5031	0.6994	0.7525

4.4.2 Synthetic Data

The hard part of evaluation is that we can't access the ground truth of the influence network from public group chat logs. To illustrate that the proposed methods can precisely extract the underlying influence network from observed chat sequences, we first conduct a set of experiments in synthetic group chat generated from well-known dialogues data. We applied Ogata's thinning algorithm to simulate a multi-dimensional Hawkes process and get the trigger of each event from previous events[86]. After we have timestamp and user for each event in simulated Hawkes process, we further embed dialogues texts from some well-known open source chitchat data to create synthetic group chat. In the simulated Hawkes process, if a user d_1 reply to user d_2, the text embedded for d_1 should be a replied text for d_2's text in dialogue chitchat.

Here, we consider a n-dimensional Hawkes process. We random select n from 4 to 1000 for 100 times. We have n users in a group, d_1, d_2, d_3 .... d_n. In particular, we consider two different types of influence matrix A in our experiments.

- **Random Relationship** For a random relationship case, we generate a matrix A where α_{ij} is sampled randomly from [0,1] for $i! = j$. The exogenous base intensity of each user is set to 0.01.
- **Sub Group Relationship** For sub group relationship case, we will assume there are 2 sub groups during n users. Users d_1 to $d_{n/2}$ are closely connected. User $d_{n/2+1}$ to d_n are close friends as another sub group. We assign high value to influence inside each sub group. We also assign low value to influence between users in different sub groups. Here we will simulate 2 Hawkes Process at the same time with an influence matrix

A. These two Hawkes Process start with users from different groups. As a result, we generate group chats where two conversations are mixed together.

Dialogue Datasets In generated data, we utilize some public dialogue datasets to create conversations inside synthetic group chat. The datasets we applied in our experiments are the same datasets we used to train the dialogue classifier, including BSTalk, ConvAI, CMUDoG, DSTC7 and PersonaChat(PC).

Evaluation Metric We use two evaluation metrics to measure the performance:

- **AveErr** AveErr is defined as average error between real influence weight and the extracted influence matrix. $i.e. \frac{\alpha ij - \alpha' ij}{\alpha ij}$ for $\alpha ij \neq 0$
- **PearsonCor** PearsonCor is defined as averaged Pearson correlation coefficient between real influence matrix A and extracted influence matrix A' , which meansures the linear correlation between αij and $\alpha' ij$

Models We extracted an influence matrix with four different models and compared the results. Here are the methods we applied to

- **TimeWindow(TW)** We set a fixed length time window. An influence weight α_{ij} is calculated based on the number of times user j speaks after user i within the fixed time length.
- **NR** NR is the number of replies. Based on the reply embedding. A influence weight α_{ij} is calculated based on the total reply embedding between user j and user i
- **MHP** MHP represents the Multi-dimensional Hawkes Process. This method will model message sequences in a group chat to a multi-dimensional Hawkes process and learn the Granger causality between different individuals by expectation-maximization algorithm
- **TTMHP** TTMHP represents the Temporal-Textual Multi-dimensional Hawkes Process. This is our proposed method in this paper which embed the text information of group chat into the multi-dimensional Hawkes process

Table (4.3) Experiments Result

Matrix	Type	Method	BSTalk	ConvAI	CMUDog	DSTC7	PC
AveErr	Random	TW	0.942	0.964	0.977	0.947	0.965
		NR	0.988	0.959	0.956	0.936	0.932
		MHP	0.407	0.369	0.511	0.443	0.492
		TTMHP	**0.399**	**0.368**	**0.486**	**0.352**	**0.422**
	Subgroup	TW	0.866	0.859	0.857	0.842	0.845
		NR	0.890	0.919	0.930	0.922	0.899
		MHP	0.625	0.610	0.576	0.631	0.625
		TTMHP	**0.289**	**0.425**	**0.295**	**0.326**	**0.384**
PearsonCor	Random	TW	0.697	0.546	0.488	0.665	0.558
		NR	0.769	0.704	0.583	0.787	0.692
		MHP	0.734	0.761	0.616	0.745	0.713
		TTMHP	**0.867**	**0.947**	**0.940**	**0.861**	**0.938**
	Subgroup	TW	0.584	0.577	0.522	0.549	0.529
		NR	0.980	0.851	0.891	0.955	0.841
		MHP	0.366	0.147	0.430	0.291	0.216
		TTMHP	**0.996**	**0.947**	**0.966**	**0.952**	**0.943**

Table 4.3 shows the average error and average Pearson correlation coefficient from our experiments. From the result, we can see our proposed model, Temporal-Textual Multi-dimensional Hawkes Process, achieves lowest error and highest correlation coefficient with these five group chat logs generated by different types of dialogues.

For random relationship group chat, we can see Hawkes process model including MHP and TTMHP get better results compared to Time window model and NR model. The time window model can capture the influence based on timestamp. NR model is calculated based on reply embedding. The performance of Hawkes process model implies that the Hawkes Process can successfully extract the trigger pattern between utterances in group chat.

For the sub group relationship case, our proposed TTMHP model still achieves the best result. Model NR is better than MHP in Pearson correlation coefficient. The reason is that model NR can capture the text information in group chat. When the group chat data is a combination of several sub groups, some close posts in a group chat could belong to different topics. Models like NR and TTMHP that utilize text information can extract

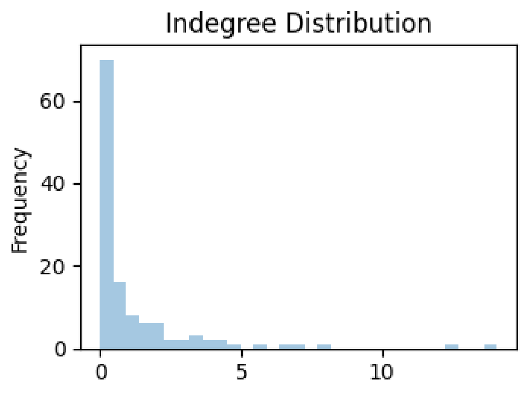

(a) node in-degree distribution

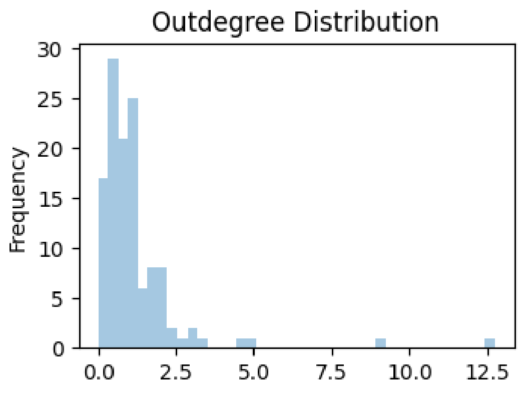

(b) node out-degree distribution

Figure (4.1) In-degree Distribution and Out-degree Distribution of an Telegram Group Chat Channel

subgroup relationships better than models like Time window and MHP that only utilize time difference.

4.4.3 Telegram Data and Case Study

To better understand the performance of the Temporal-Textual Multi-dimensional Hawkes Process model on real data, we apply our proposed model to chat logs from telegram group channels.

For the influence network we extracted, most members only interact with a few members or don't interact with others in the group. Figure 4.1 shows the influence's in-degree distribution and out-degree distribution of an example channel in telegram. We can tell most people have low influence on others, which matches the reality that most people don't know each other in an online chat group.

Figure 4.2 shows an infectivity network of a 30 members group channel. In this graph, each node represents a user in this group and a directed weighted edge represents the influence between users. To provide a more straightforward insight of the influence network, we let the width of the edge proportional to influence coefficient and size of node proportional to in-degree of influence. Here yellow nodes represent the normal members in this group and the red node "Guitar" represents the administrator of this group. From this graph, node

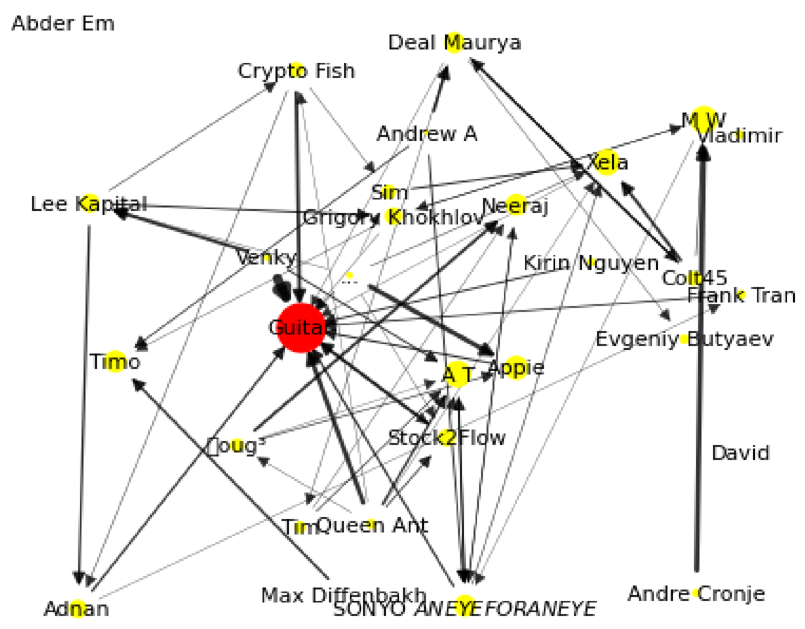

Figure (4.2) Influence Network of an 80 Members Telegram Channel

”Guitar” has the maximum in-degree influence. By checking the chat history of this group, we found that the user ”Guitar” answered a lot of questions and helped other members in this group. This indicates the influence graph can reflect the trigger pattern of this group chat. Such kind of information can provide investigative insight for law enforcement to analyze the organization structure of members in these online groups.

4.5 Conclusion

In this paper, we study the problem of learning infecivity graph from group chat logs. We firstly implement a dialogue classifier which can classify whether the second text is a reply for the first text semantically when we input two sentences. We convert the group chat log to an event sequence where every utterance is an event and the member who post this message is the event type. We model the event sequence with multi-dimensional Hawkes process and embed the text information we extracted through the dialogue classifier to kernal function of the Hawkes process model. By applying an EM algorithm, we successfully extract the trigger pattern between members inside a group channel. Comprehensive experimental results show the effectiveness and efficiency of the proposed methods.

PART 5

CLUSTERING OF ACCOUNTS IN ONLINE MESSAGING SOFTWARE THROUGH ATTRIBUTED HETEROGENEOUS INFORMATION NETWORKS

In this part, we propose an effective model to learn the embedding of each account in group chat. We further train a classifier to identify accounts that belong to the same user.

5.1 Motivation

The privacy of participants in illicit online transactions is protected through two parts. One is the platform where vendors sell their products and the other is the emergence of cryptocurrency.

Instant Message software like Telegram, providing public channels for users to discuss and conduct illegal activities[9, 53], become one of biggest platforms for illicit sales.

Telegram offers users a completely free open-source platform without any ads, a clean interface, and (the biggest selling point) security[87]. One important feature of Telegram is being able to search the channels posts, group messages, individual messages or any kind of communications or posts. This feature is available for both cell phone applications and the Web-based Telegram interface making it possible to reach any content by simply searching[88, 89]. This essentially makes Telegram one of the largest free databases available to the public, especially considering the fact that many other media outlets, including Google, Instagram, Twitter, and Facebook, are constantly removing illegal posts. Even though there are illegal activities in these chat channels, administrators of these group channels still keep these channels public to let new buyers and vendors join the channel easily. Users of Telegram can search product names in Telegram and they are able to find related chat channels easily without any effort. Figure 5.1 shows the result of searching the keyword "silkroad" in

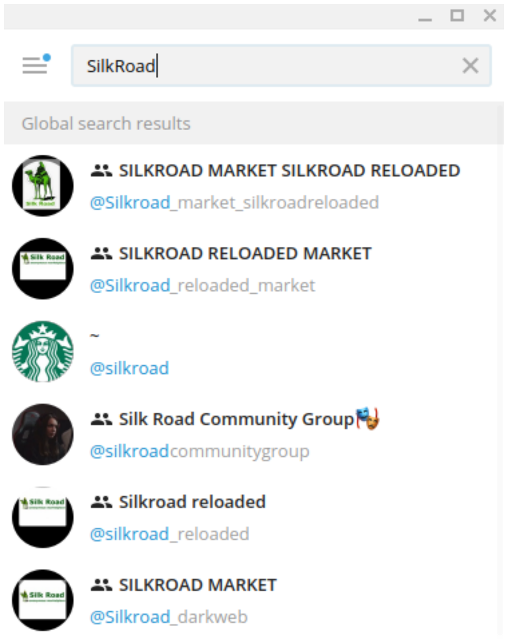
SilkRoad

Global search results

SILKROAD MARKET SILKROAD RELOADED
@Silkroad_market_silkroadreloaded

SILKROAD RELOADED MARKET
@Silkroad_reloaded_market

~
@silkroad

Silk Road Community Group
@silkroadcommunitygroup

Silkroad reloaded
@silkroad_reloaded

SILKROAD MARKET
@Silkroad_darkweb

Figure (5.1) Searching SilkRoad in Telegram

Telegram. SilkRoad is one of the most famous darknets that sell drugs[90]. After joining these channels, buyers can see the vendors posts about their products in the chat channel and vendors can advertise their products periodically. If the buyer is interested in the product posted by the vendor, he or she can discuss details with the vendor in the group channel or create a private chat channel with the vendor.

To combat these illegal sales, it's critical for law enforcement to know the organizations of users in these group chat channels and analyze influence networks. However, no matter vendors or buyers, they normally maintain multiple accounts in the Telegram platforms. To track the ecosystem of users and build a network of the users, it's critical that we are able to link different accounts belonging to the same user.

Given the large number of users and millions of chat logs, it's impossible to manually label accounts of the same user and cluster them. Therefore, there is an urgent need to develop a model which can automatically identify accounts belonging to one user or different users.

The remainder of this paper is organized as follows. Section 2 review related work, followed by the proposed methods in Section 3. Section 4 details our experiments. Section 5 shows case study and section 6 concludes the paper.

5.2 Related Work

We perform a literature review focusing on the following two aspects: 1) Study on Telegram data 2) Time series data representation learning. 3) Graph Node representation learning

5.2.1 Telegram

Telegram is an instant message application that can be accessed by a wide range of users. To protect user's privacy, Telegram provides encryption services for their customers, which can prevent potential eavesdroppers – including software developers and internet providers. However, these privacy-protecting and convenient software has been utilized by criminals for illegal activities like drug smuggling, online fraudulence or even anti-social activities[9]. In recent years, a lot of works analyze the criminal activities data from Telegram[89, 91–93].

Anglano presents a methodology for the forensic analysis of the artifacts generated on Android smartphones by Telegram Messenger[91]. Their methodology is based on the design of a set of experiments suitable to elicit the generation of artifacts and their retention on the device storage. Satrya also presents a thorough description of all the artifacts that are generated by the messenger application Telegram on Android OS[92]. Gregorio did similar work for Windows phone, focusing particularly on how the information is structured and the user, chat and conversation data generated by the application are organized, with the goal of extracting related data from the information[93]. However, none of these works are trying to identify different accounts that are managed by the same user.

5.2.2 Time Series Representation Learning

The aim of time series representation learning is to learn the embedding of time series data that can be used to measure the similarity of two time series data. Learning universal representations for time series is a fundamental but challenging problem.

Yue presents TS2Vec, a universal framework for learning representations of time series in an arbitrary semantic level. Unlike existing methods, TS2Vec performs contrastive learning in a hierarchical way over augmented context views, which enables a robust contextual representation for each timestamp.[94]. Lei proposing an efficient representation learning framework that is able to convert a set of time series with various lengths to an instance-feature matrix. In particular, they guarantee that the pairwise similarities between time series are well preserved after the transformation, thus the learned feature representation is particularly suitable for the time series clustering task.[95] Eldele proposes an unsupervised Time-Series representation learning framework via Temporal and Contextual Contrasting (TS-TCC), to learn time-series representation from unlabeled data[96]. These work measure similarity of two time series data with classic methods such as Mikowski distance, cross-correlation, Kullback-Leibler divergence, dynamic time warping(DTW) similarity, move-split-merge(MSM) distance, and short time series(STS) distance. These researches focus on the time series data instead of timestamp. In our problem, we want to know the similarity of two timestamp lists, which can't be accurately measured by methods like dynamic time warping. We develop a machine learning model that can learn the representation of a time stamp list and measure the similarity between two timestamp lists through learned embedding.

5.2.3 Graph Node Representation Learning

Since most real-world data can be conveniently represented by graphs, research on graph representation learning has received increasing attention in recent years[97].

Classical graph embedding methods can be divided into linear and nonlinear categories. Linear methods include: Principal component analysis (PCA)[98], Linear discriminant anal-

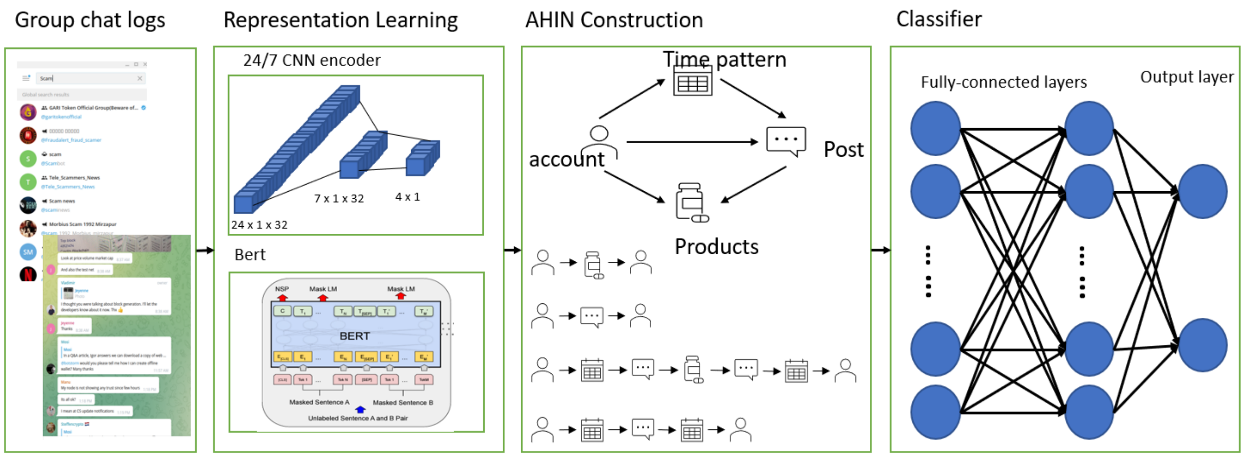

Figure (5.2) System Architecture

ysis (LDA)[99] and Multidimensional scaling (MDS)[100]. Non-linear dimensionality reduction methods include: Isometric feature mapping (Isomap)[101], Locally linear embedding (LLE)[102] and Kernel methods[103].

Random-walk-based methods sample a graph with a large number of paths by starting walks from random initial nodes. DeepWalk learns these latent representations to encode social relations in a continuous vector space. DeepWalk summarizes recent advances in language modeling and unsupervised feature learning from word sequences to graphs[104]. node2vec is a modified version of DeepWalk, which defines a flexible notion of a node's network neighborhood and design a biased random walk procedure[105]. Our node representation learning method utilizes the time pattern and text. We sample meta paths from the AHIN we built and construct biased random walks.

5.3 Proposed Method

An overview of our developed system for accounts clustering in Telegram is shown in Figure 5.2. In this section, we introduce the detailed methods integrated in the model to identify accounts belonging to the same user.

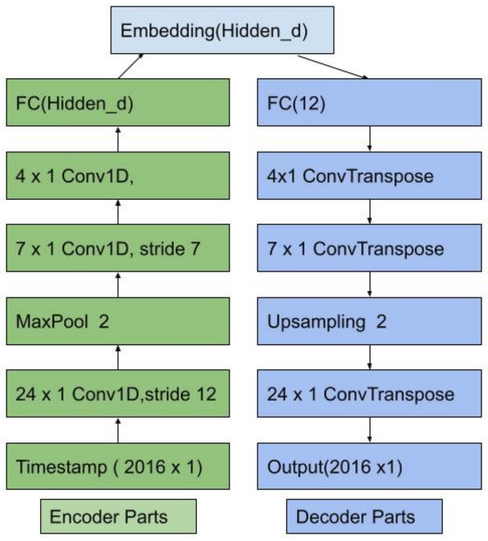

Figure (5.3) Auto-encoder Structure

5.3.1 Time Pattern Representation Learning

To construct an attributed network, the first step is to learn the attribution for each node. For node type ”time pattern”, we need to learn the hidden properties of each timestamp list.

From telegram chat logs, we are able to extract posts of each account as well as timestamp of each post. Accounts belonging to one user should display similarities in time pattern for post. The similarity is not just measured by the Euclidean distance of two timestamp lists. User’s time zone, location, work routine may affect the timestamp list. For example, some users prefer to post in the morning, some may prefer night and some may only work on weekdays. There also might exist some relationships between timestamps of user’s different posts. To gather all of this information into a relational vector whose distance can represent the similarity level is not an easy task.

In this paper, we propose to build an auto-encoder to learn the hidden properties of these timestamp lists because we don’t have enough labeled data. Different from other dimensionality reduction methods, auto-encoder not only reduces dimensionality, but can also detect repetitive structures[106]. We believe this is a good property for our situation. Users post the advertisements of their products repeatedly in group chat channels.

In the encoder part, we tried different types of neural networks and experiments in part 4 shows convolutional neural network encoders perform best among all these types of encoders. CNNs were well known in the computer vision and machine learning communities[107]. AlexNet shows, for the first time, that the features obtained by learning can transcend manually-designed features, breaking the previous paradigm in computer vision. [108].Our CNN encoder shows similar design philosophies with AlexNet.

Figure 5.3 shows the details of each layer in encoder and decoder. First of all, We preprocess each timestamp list to a vector. Here we only record the timestamp list of each account from the last 3 month. In total there are 12 weeks which are 2016 hours long. We use a 2016×1 vector to represent the timestamp list, each value in this vector is the number of posts in that hour. Hour is the smallest time unit we would consider. In our encoder, we have convolutional layers, max pooling layer and fully connected layer. In the first convolutional layer, we set the filter's size as 24 which can convolute timestamps in consecutive 24 hours. After the max pooling layer, each data is the learned embedding of one day long. The second convolutional layer's filter size is 7, which will convolute timestamps in a week. Followed by the last convolutional layer which will convolute timestamps in 4 weeks. Decoder's designs are opposite layers of related encoder layers.

By training the auto-encoder, we get the hidden features we want to measure the similarity of the timestamp list. The encoder is the model we want to utilize to learn the representations of timestamp lists. We can get the low dimensional embedding of each timestamp list by process timestamp list through the learned encoder.

5.3.2 Text Features Extractions

Except for the time pattern, our model leverages the text post by the account as well. Therefore we also need to learn the representations of post text in group chat channels.

In this paper, we learn the representation of text by a pre-trained language model, BERT. BERT is designed to pre-train deep bidirectional representations from text by jointly conditioning on both left and right context in all layers[79]. It's empirically powerful and has obtained state-of-art results on several natural language processing tasks. We input one text to a pre-trained BERT model which converts text to a vector.

5.3.3 AHIN Construction

To describe vendors, time patterns, texts, product-related attributes, and the rich relationships between them, we propose to use the attributed Attributed Heterogeneous Information Network (AHIN) for representation.

Attributed Heterogeneous Information Network (AHIN)[109]: Let $\mathcal{T} = \{T_1, ..., T_m\}$ be a set of m object types. For each type T_i, let $\mathcal{X}_i$ be the set of objects of type T_i and A_i be the set of attributes defined for objects of type T_i. An object x_j of type T_i is associated with an attribute vector $f_j = (f_{j1}, f_{j2}, ..., f_{j|A_i|})$. An AHIN is a graph $G = (V, E, \mathcal{A})$, where $V = \cup_{i=1}^{m} \mathcal{X}_i$ is a set of nodes, E is a set of edge, each represents a binary relation between two objects in V , and $\mathcal{A} = \cup_{i=1}^{m} A_i$.

To better understand the schema level of the AHIN we built, we provide a meta-level description.

Network Schema[109, 110]: A network schema is the meta template of an AHIN $G = (V, E, \mathcal{A})$. Let (1) $\psi : V \to \mathcal{T}$ be an object-type mapping that maps an object in V into its type, and (2) $\psi : E \to \mathcal{R}$ be a link-relation mapping that maps a link in E into a relation in a set of relations $\mathcal{R}$. The network schema of an AHIN G, denoted by $T_G = (\mathcal{T}, \mathcal{R})$, shows how objects of different types are related by the relations in $\mathcal{R}$. T_G can be represented by a schematic graph with $\mathcal{T}$ and $\mathcal{R}$ being the node set and the edge set, respectively. Specifically, there is an edge (T_i, T_j) in the schematic graph iff there is a relation in $\mathcal{R}$ that relates objects of type T_i to objects of type T_j .

Figure 5.4 shows the network schema of our application. In our network, we have four node types and five binary relations. Two accounts can be connected via different paths through our heterogeneous network.

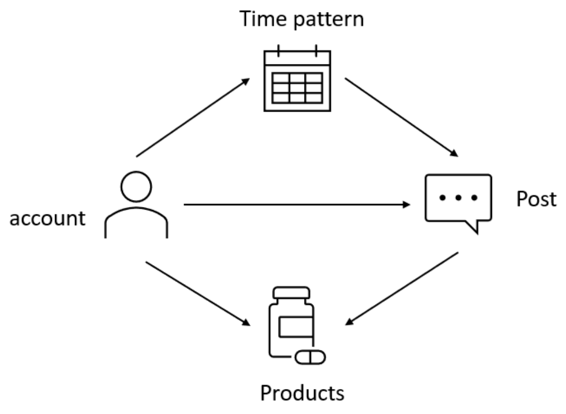

Figure (5.4) Network Schema

Meta path P is a path defined on the graph of network schema T_G [111], which include types, nodes and relations. A meta path is symmetric if the relation defined by it is symmetric.

In our application, we are able to find the same text post by different accounts or same products by different accounts. Therefore, we can create symmetric meta paths with product nodes or post nodes as bridges. Figure 5.5 shows the four most meaningful symmetric meta paths we applied to present relationships between two accounts in Telegram from different views. **MP1** means two accounts are connected by posting the same product in the Telegram group chat channel. **MP2** means two accounts are connected by posting the same text. **MP3** denote that two accounts can be linked if they posted the text describing the same product with similar time pattern. **MP4** represents that two accounts can be linked if they post the same text with similar timestamps.

5.3.4 The User2Vec Model

We present a framework, User2Vec, which is capable of learning account representations in the attributed heterogeneous network we built. The desirable node representations should be low dimensional and preserve the context of each node in the heterogeneous network.

Given a heterogeneous network as input, we formalize the problem of heterogeneous

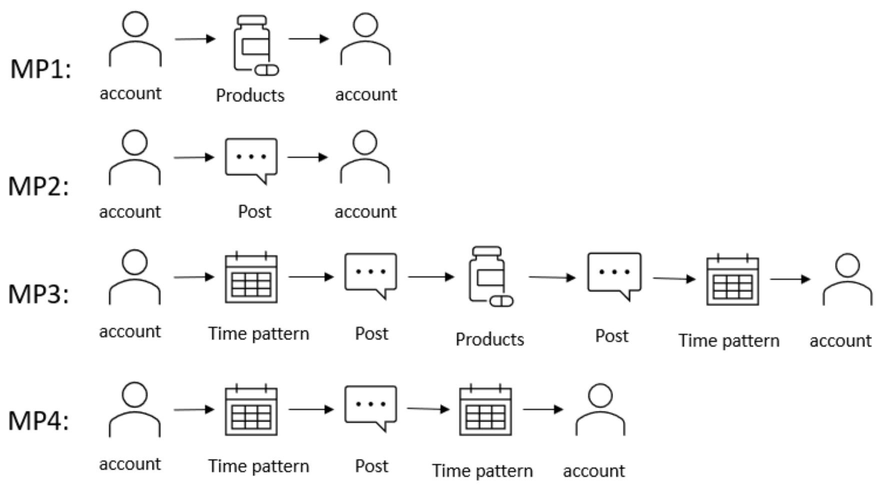

Figure (5.5) Meta path

network representation learning as follows.

Attributed Heterogeneous Network Representation Learning[112]: Given a heterogeneous network $\mathcal{G} = (\mathcal{V}, \mathcal{E}, \mathcal{A})$, the task is to learn the d-dimensional latent representations $R^{|\mathcal{V}| \times d}$, $d \ll |\mathcal{V}|$ that are capable of capture the structural and semantic relations among them.

We first introduce the embedding method for homogeneous networks and heterogeneous networks. Mikolov et al. proposed Word2Vec which can learn the embedding of each word from the context in a given text corpus[113]. By applying the same idea, DeepWalk and Node2vec learn the node embedding from the context of each node in network [104]. Both methods sample paths from the network through random walks and transfer the network structure into a skip-gram model and embed the nodes to the low dimensional vectors. To learning the embedding of heterogeneous network with similar solution, metapath2Vec extracts the path from meta path of heterogeneous network[112]

In our application, we want to leverage the attribute vector of time pattern and text nodes. We apply a biased meta path method to guide attributed heterogeneous random walks. Given a attributed heterogeneous network $G = (\mathcal{V}, \mathcal{E}, \mathcal{A})$ and a meta-path scheme

$\mathcal{P} : T_1 \rightarrow T_2 \rightarrow \cdots T_t \rightarrow T_{t+1} \cdots \rightarrow T_l$, the transition probability at step i is defined as:

$$p(v^{i+1}|v_t^i, \mathcal{P}) = \begin{cases} \frac{sim(f_{v'}, f_{v^{i+1}})}{\sum_{v^c \in N_{T_{t+1}}(v_t^i)} sim(f_{v'}, f_{v^c})} & (v_t^i, v_{i+1}) \in \mathcal{E}, \psi(v^{i+1}) = T_{t+1}, v\prime \text{exists} \\ \frac{1}{N_{T_{t+1}}(v_t^i)} & (v_t^i, v_{i+1}) \in \mathcal{E}, \psi(v^{i+1}) = T_{t+1}, v\prime \text{not exists} \\ 0, & (v^{i+1}, v_t^i) \notin \mathcal{E} \end{cases}$$

where v_i represents the the node visited in i^{th} step and $N_{T_{t+1}}(v_t^i)$ represents the T_{t+1} type neighbor nodes of v_i. In our application, we sample paths from symmetric meta path. If v_i in the first half of meta path, the probability of transition to node in type T_{t+1} is inversely proportional to number of neighbors in type T_{t+1}. If v_i in the second half of meta path, then a symmetric node of v^{i+1} exists, which is v' in our equation. Here we need to calculate the similarity of v^{i+1} and v'. $sim(f_{v'}, f_{v^{i+1}}$ is the similarity calculated by attribute vector of node v' and node v^{i+1} A node with higher similarity with v' will be sampled with higher possibility in random walk. With this guide, we can generate node sequences which can be the input of skip-gram model.

5.3.5 Classification Model

In the end of our model, we feed a pair of account vectors to a binary classifier.

We apply a Deep neural network into account embedding, which contains fully connected layers. The last layer includes two neurons to decide whether the pair of accounts are from the same user.

5.4 Experiments and Results

In this section, we first compare the performance of representation learning of auto-encoders. Followed by the evaluation of User2Vector in Attributed Heterogeneous Information Network.

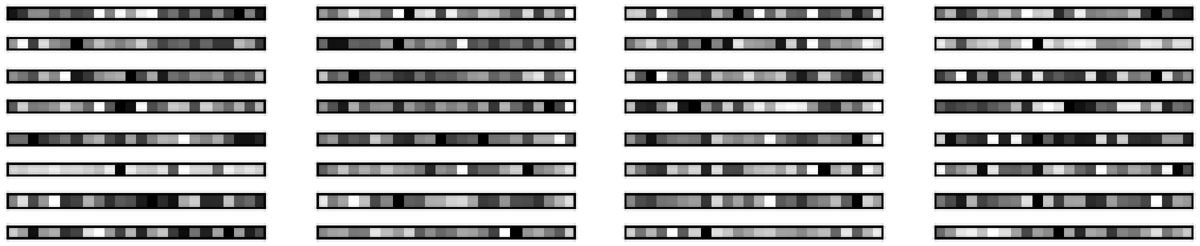

Figure (5.6) Filters Learned by the First Layer of 24-7CNN

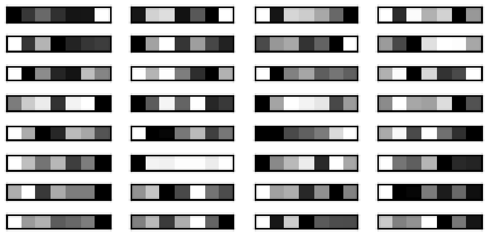

Figure (5.7) Filters Learned by the Second Layer of 24-7CNN

5.4.1 Time Pattern Embedding Comparisons

In this set of experiments, we first evaluate the effectiveness of CNN encoder as a representation learning model.

To fully evaluate the representation learning method, we have downloaded the data from popular Telegram public channels. We develop a related parser to parse the timestamp list of each account from Jan-3-2022 to Mar-27-2022. Here we parsed 161797 posts from 7569 accounts. If the timestamp list is too short, we are not able to learn the features of a time pattern. Therefore, we remove accounts that post less than 10 times.

Due to the anonymity of Telegram, we don't know which ones are owned by the same user. After we train the encoders with a parsed timestamp list, we randomly separate the timestamp list of each account into two sublists equally. By comparing the similarities between those sublists, we are able to evaluate the effectiveness of the learned encoder.

Here we compare four types of encoder and manually-designed features.

Models Here we compare four types of encoder and manually-designed features

- **CNN auto-encoder** Details of encoder and decoder design are displayed in Figure 5.3. In our encoder, we have convolutional layers, max pooling layer and fully connected layer. Decoder's designs are opposite layers of related encoder layers.
- **RNN auto-encoder** RNN auto-encoder's design is similar to the CNN auto-encoder, where we replace convolutional layers with simple RNN layers.
- **LSTM auto-encoder** LSTM auto-encoder's design is similar to the RNN auto-encoder, where we replace simple RNN layers with LSTM layers.
- **FC auto-encoder** FC represents a fully connected layer. In FC encoder, we have three layers of fully connected neural networks.
- **Manually-designed Features** We also test the manually selected features. In our design, each timestamp list is converted to a $24+7 = 31$ dimensional vector. It includes the number of posts in 24 separate hours and number of posts from Monday to Sunday.

DataSets Here we use 2 types of data

- **Telegram Data** We parse the timestamp list of each account from Jan-3-2022 to Mar-27-2022 and randomly separate the timestamp list into two sublists.
- **Synthetic** For each timestamp list we parse from Telegram, we create a synthetic timestamp list. We manually replace each timestamp with a random hour in the same day or same hour on a random day of this week.

Evaluation Metric The aim of our experiments are trying to see whether the learned embedding can be used to measure the similarities of timestamp lists. Consider the learned embedding of these models in different scales. Here we use the percentage value as an evaluation metric instead of Euclidean distance of vectors. We first set a threshold $\lambda\%$. Here we calculate the Euclidean distance between learned vectors and link each account with the top nearest $\lambda\%$ accounts. We use the percentage of successful linkage as Evaluation Metric.

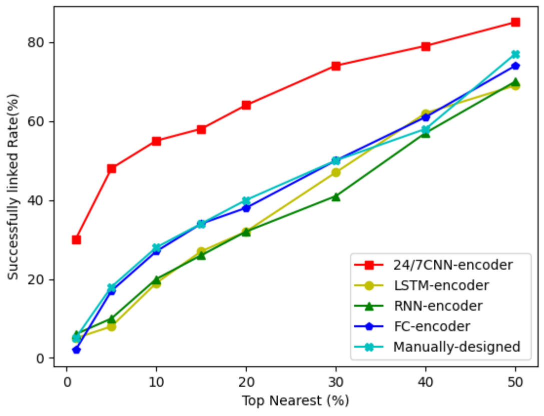

(a) on real data

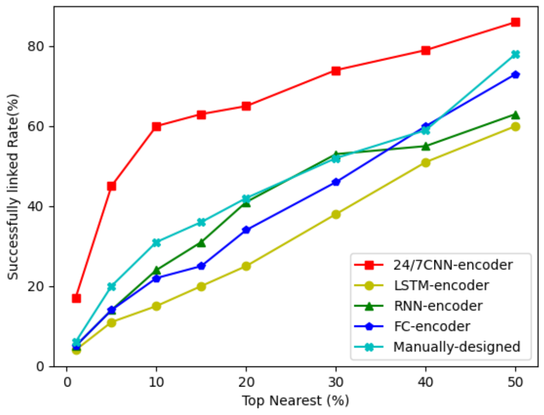

(b) on synthetic data

Figure (5.8) Comparisons of Embedding

Figure 5.3 shows the experiment's result. We start from λ%, which means we link each account with λ% nearest 1% accounts. We can see embedding learned by CNN encoder can successfully link 28% of all account pairs, which is much higher than the result from RNN encoder, LSTM encoder, Fully-Connected encoder and manually designed features.

To get the intuitive sense of embedding of CNN encoder. We convert a vector of 20 pairs accounts into a 2 dimensional vector. Figure 5.9 shows the result and we can see accounts from the same user are close to each other.

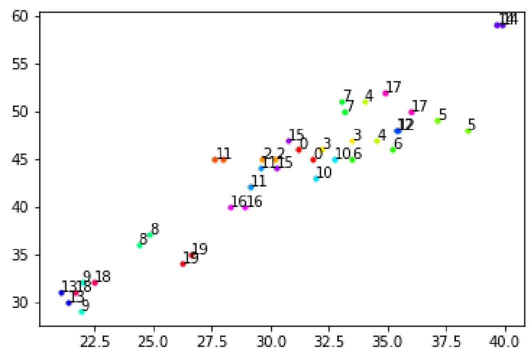

(a) on real data

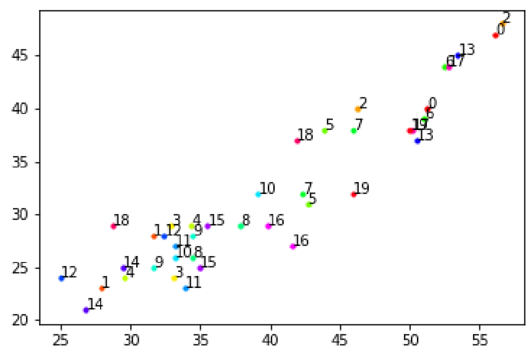

(b) on synthetic data

Figure (5.9) Learned Representation of 24/7 CNN Encoder

5.4.2 User2Vec Performance

To evaluate the performance of our System, we compare three different networks. Not only the attributed heterogeneous network, we also build heterogeneous network and homogeneous network with the same data.

For the heterogeneous network, we didn't attach attributes for timestamp nodes or post type nodes. We use metapath2Vec to sample the path from the network, which will sample meta paths we extracted from the network schema, however, the possibility of the next node will not be affected by the attributed vector [112].

For the homogeneous network, we treat all the nodes as the same type and we sample the paths with DeepWalk which utilizes random walkers without following any meta paths[104].

We compare the performance of these three models with two community data from telegram. One is scam related channels and another one is drug related channels.

Table (5.1) Comparisons of Different Models

Channels	AHIN+ User2Vec	HIN+ metepath2Vec	Homo network+ DeepWalk
Scam	0.785	0.696	0.6875
Drug	0.8025	0.713	0.694

Table 5.1 shows the accuracy of trained classifiers of three different models. We can see that our model which leverages most information from the network can achieve the best accuracy.

5.4.3 Case Study

Table (5.2) Post Frequency of Account1 and Account2

Account1		Account2	
date and time	Frequency	date and time	Frequency
04/16, 9pm	9	04/14, 8pm	5
04/16, 10pm	5	04/14, 9pm	10
04/16, 11pm	26	04/14, 10pm	7
04/17, 12am	12	04/14, 11pm	3
04/17, 1am	11	04/15, 12am	2
04/17, 2am	5	04/15, 1am	8
		04/15, 2am	4
		04/15, 10pm	1
		04/15, 11pm	12
		04/16, 12am	15
		04/16, 1am	6
		04/16, 9pm	4
		04/16, 10pm	1
		04/17, 12am	5

We also tried unlabeled data from telegram to gain deeper insights of our proposed model. For the pairs of accounts that are defined as one user, we are with high confidence

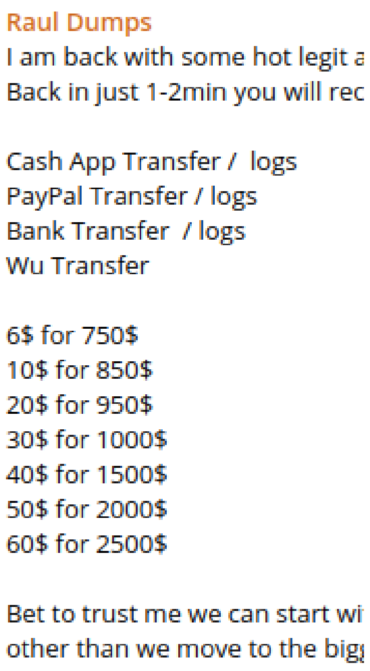

Raul Dumps
I am back with some hot legit a
Back in just 1-2min you will rec

Cash App Transfer / logs
PayPal Transfer / logs
Bank Transfer / logs
Wu Transfer

6$ for 750$
10$ for 850$
20$ for 950$
30$ for 1000$
40$ for 1500$
50$ for 2000$
60$ for 2500$

Bet to trust me we can start wi
other than we move to the big

(a) Post of Account1

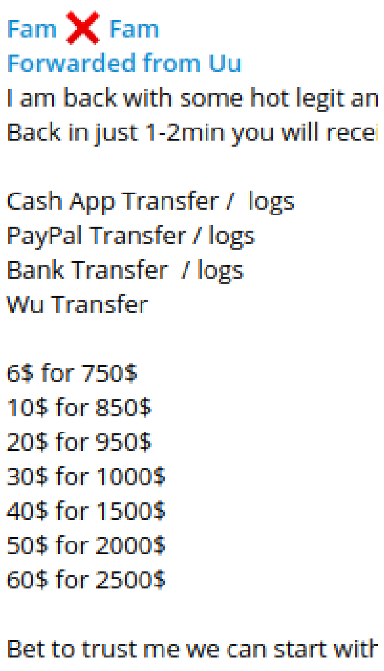

Fam ❌ Fam
Forwarded from Uu
I am back with some hot legit an
Back in just 1-2min you will rece

Cash App Transfer / logs
PayPal Transfer / logs
Bank Transfer / logs
Wu Transfer

6$ for 750$
10$ for 850$
20$ for 950$
30$ for 1000$
40$ for 1500$
50$ for 2000$
60$ for 2500$

Bet to trust me we can start with

(b) Post of Account2

Figure (5.10) Post Text of Detected Account Pair Account1 and Account2

that they are the same individual by manually checking. For example, Figure 5.10 shows the post by these two accounts, we can see the text is extremely similar. Both accounts post a lot of times. To better show the timestamp list, we count the frequency of posts in each hour and display the result in Table 5.2. We can tell these two accounts are very active from 10pm to 3am.

5.5 Conclusion

In this paper, we study the problem of how to identify the accounts from the same user in Messaging Software. After we parse the chat logs from public channels, we first extract the features of the timestamp list and text post of each account. We learn the embedding of timestamp list through a novel 24/7 CNN encoder and the embedding of post through pre-trained self attention transformer Bert. We further proposed the User2Vec model, where we sample the meta path from AHIN we build and feed the paths that capture the structure and semantic relations to the skip-gram model. In the end, we train a binary classifier to classify each pair of accounts to decide whether they are the same user or not. Comprehensive experimental results have demonstrated the effectiveness and efficiency of the proposed model.

PART 6

CONCLUSION

In this dissertation, we present our research on how to combat cyber crime by attacking privacy provided by darknet and IM softwares.

For darknet, we firstly analyze Bitcoin transaction patterns behind cryptomarkets and discover interesting transaction patterns and management mechanisms from different cryptomarkets. The results demonstrate that the privacy protection mechanism in Bitcoin is still vulnerable in terms of simple analysis. For markets like the Wall Street market, feedback reviews released on web pages are highly related with public Bitcoin transactions in terms of timestamp and money value. An adversary can extract valuable information for analyzing the activities. Based on the transactions pattern we discovered from darknet markets, we further proposed a method to uncover the Bitcoin addresses of a vendor in darknet by matching their feedback reviews with public bitcoin transactions. We first proposed the metric which is maximum coverage of reviews by a Bitcoin address. A Bitcoin address's transaction history can match maximum reviews owned by the vendor with the highest possibility. In our model, we construct a K-D tree to efficiently match Bitcoin transactions to feedback reviews based on timestamp and money value. The problem is proved to be NP hard. By utilizing the sub modular property of our objective function, we get the address set with a greedy algorithm that can achieve near-optimal with theoretical guarantee. We further develop a Cost-Effective Address Searching(CEAS) algorithm that can speed up the process by pruning the search space effectively. Comprehensive experiments on both real and synthetic datasets demonstrate the effectiveness and efficiency of our methods.

For IM software like telegram, vendors broadcast their products through related group chat. A group in such IM softares normally contains thousands of members including both vendors and customers. Learning infectivity graphs from these group chats can help us analyze organizations and supply chains behind these illegal products. We propose an effective model to discover hidden networks of influence between members in a group chat. We model message sequences to a multi-dimensional Hawkes process by treating the whole chat history as sequential events. The triggering pattern between members inside a group can help us extract influence between different individuals. In our model, we apply NLP techniques to embed the text information of messages to get a more precise relationship between members in group chat. We learn the influence graph by applying an expectation–maximization(EM) algorithm on our text biased multi-dimensional Hawkes Process. And we conduct experiments with designed metrics on synthetic data and real data with different models.

We further study the problem of how to cluster the accounts from the same user in Messaging Software. We learn the embedding of timestamp list through a novel 24/7 CNN encoder and the embedding of post through pre-trained self attention transformer Bert. We further proposed the User2Vec model, where we sample the meta path from AHIN we build and feed the paths that capture the structure and semantic relations to the skip-gram model. In the end, we train a binary classifier to classify each pair of accounts to decide whether they are the same user or not.

REFERENCES

[1] J. Van Buskirk, S. Naicker, A. Roxburgh, R. Bruno, and L. Burns, “Who sells what? country specific differences in substance availability on the agora cryptomarket,” *International Journal of Drug Policy*, vol. 35, pp. 16–23, 2016.

[2] S. Nakamoto, “Bitcoin: A peer-to-peer electronic cash system,” Manubot, Tech. Rep., 2019.

[3] F. Reid and M. Harrigan, “An analysis of anonymity in the bitcoin system,” in *Security and privacy in social networks*. Springer, 2013, pp. 197–223.

[4] R. Böhme, N. Christin, B. Edelman, and T. Moore, “Bitcoin: Economics, technology, and governance,” *Journal of economic Perspectives*, vol. 29, no. 2, pp. 213–38, 2015.

[5] S. Kethineni, Y. Cao, and C. Dodge, “Use of bitcoin in darknet markets: Examining facilitative factors on bitcoin-related crimes,” *American Journal of Criminal Justice*, vol. 43, no. 2, pp. 141–157, 2018.

[6] S. Lee, C. Yoon, H. Kang, Y. Kim, Y. Kim, D. Han, S. Son, and S. Shin, “Cybercriminal minds: an investigative study of cryptocurrency abuses in the dark web,” in *Network and Distributed System Security Symposium*. Internet Society, 2019, pp. 1–15.

[7] S. Underwood, “Blockchain beyond bitcoin,” 2016.

[8] G. Hileman and M. Rauchs, “Global blockchain benchmarking study,” *Rochester, NY: Social Science Research Network*, 2017.

[9] J. Bengel, S. Gauch, E. Mittur, and R. Vijayaraghavan, “Chattrack: Chat room topic detection using classification,” in *International Conference on Intelligence and Security Informatics*. Springer, 2004, pp. 266–277.

[10] "How bitcoin lets you spy on careless companies," https://web.archive.org/web/20140209202222/http://www.wired.co.uk/news/archive/2013-06/06/bitcoin-retail, accessed: 2019-03-10.

[11] "Mapping the bitcoin economy could reveal users' identities," https://www.technologyreview.com/s/518816, accessed: 2019-03-10.

[12] "Five surprising facts about bitcoin," https://www.washingtonpost.com/news/the-switch/wp/2013/08/21/five-surprising-facts-about-bitcoin, accessed: 2019-03-10.

[13] D. Ron and A. Shamir, "Quantitative analysis of the full bitcoin transaction graph," in *International Conference on Financial Cryptography and Data Security.* Springer, 2013, pp. 6–24.

[14] E. Androulaki, G. O. Karame, M. Roeschlin, T. Scherer, and S. Capkun, "Evaluating user privacy in bitcoin," in *International Conference on Financial Cryptography and Data Security.* Springer, 2013, pp. 34–51.

[15] M. Spagnuolo, F. Maggi, and S. Zanero, "Bitiodine: Extracting intelligence from the bitcoin network," in *International Conference on Financial Cryptography and Data Security.* Springer, 2014, pp. 457–468.

[16] M. Fleder, M. S. Kester, and S. Pillai, "Bitcoin transaction graph analysis," *arXiv preprint arXiv:1502.01657*, 2015.

[17] M. Harrigan and C. Fretter, "The unreasonable effectiveness of address clustering," in *2016 Intl IEEE Conferences on Ubiquitous Intelligence & Computing, Advanced and Trusted Computing, Scalable Computing and Communications, Cloud and Big Data Computing, Internet of People, and Smart World Congress (UIC/ATC/ScalCom/CBDCom/IoP/SmartWorld).* IEEE, 2016, pp. 368–373.

[18] T. Ruffing, P. Moreno-Sanchez, and A. Kate, "Coinshuffle: Practical decentralized

coin mixing for bitcoin," in *European Symposium on Research in Computer Security.* Springer, 2014, pp. 345–364.

[19] J. H. Ziegeldorf, F. Grossmann, M. Henze, N. Inden, and K. Wehrle, "Coinparty: Secure multi-party mixing of bitcoins," in *Proceedings of the 5th ACM Conference on Data and Application Security and Privacy.* ACM, 2015, pp. 75–86.

[20] M. Gilbert and N. Dasgupta, "Silicon to syringe: Cryptomarkets and disruptive innovation in opioid supply chains," *International Journal of Drug Policy*, vol. 46, pp. 160–167, 2017.

[21] "Bitcoin core," https://bitcoin.org/en/bitcoin-core/, accessed: 2019-03-10.

[22] "Running a full node," https://bitcoin.org/en/full-node#what-is-a-full-node, accessed: 2019-03-10.

[23] "How to parse the bitcoin blockchain," http://codesuppository.blogspot.com/2014/01/how-to-parse-bitcoin-blockchain.html, accessed: 2019-03-10.

[24] "bitcoin-blockchain-parser," https://github.com/alecalve/python-bitcoin-blockchain-parser/blob/master/README.md, accessed: 2019-03-10.

[25] S. Nakamoto *et al.*, "Bitcoin: A peer-to-peer electronic cash system," 2008.

[26] S. Meiklejohn, M. Pomarole, G. Jordan, K. Levchenko, D. McCoy, G. M. Voelker, and S. Savage, "A fistful of bitcoins: characterizing payments among men with no names," in *Proceedings of the 2013 conference on Internet measurement conference.* ACM, 2013, pp. 127–140.

[27] D. Genkin, D. Papadopoulos, and C. Papamanthou, "Privacy in decentralized cryptocurrencies," *Communications of the ACM*, vol. 61, no. 6, pp. 78–88, 2018.

[28] T. de Balthasar and J. Hernandez-Castro, "An analysis of bitcoin laundry services," in *Nordic Conference on Secure IT Systems.* Springer, 2017, pp. 297–312.

[29] X. Chen, M. Al Hasan, X. Wu, P. Skums, M. J. Feizollahi, M. Ouellet, E. L. Sevigny, D. Maimon, and Y. Wu, "Characteristics of bitcoin transactions on cryptomarkets," in *International Conference on Security, Privacy and Anonymity in Computation, Communication and Storage.* Springer, 2019, pp. 261–276.

[30] Y. Fanusie and T. Robinson, "Bitcoin laundering: an analysis of illicit flows into digital currency services," *Center on Sanctions and Illicit Finance memorandum, January*, 2018.

[31] M. Tran, L. Luu, M. S. Kang, I. Bentov, and P. Saxena, "Obscuro: A bitcoin mixer using trusted execution environments," in *Proceedings of the 34th Annual Computer Security Applications Conference*, 2018, pp. 692–701.

[32] M. Spagnuolo, F. Maggi, and S. Zanero, "Bitiodine: Extracting intelligence from the bitcoin network," in *International Conference on Financial Cryptography and Data Security.* Springer, 2014, pp. 457–468.

[33] M. Fleder, M. S. Kester, and S. Pillai, "Bitcoin transaction graph analysis," *arXiv preprint arXiv:1502.01657*, 2015.

[34] E. Androulaki, G. O. Karame, M. Roeschlin, T. Scherer, and S. Capkun, "Evaluating user privacy in bitcoin," in *International Conference on Financial Cryptography and Data Security.* Springer, 2013, pp. 34–51.

[35] S. Meiklejohn, M. Pomarole, G. Jordan, K. Levchenko, D. McCoy, G. M. Voelker, and S. Savage, "A fistful of bitcoins: characterizing payments among men with no names," in *Proceedings of the 2013 conference on Internet measurement conference*, 2013, pp. 127–140.

[36] D. Genkin, D. Papadopoulos, and C. Papamanthou, “Privacy in decentralized cryptocurrencies,” *Communications of the ACM*, vol. 61, no. 6, pp. 78–88, 2018.

[37] M. Masoni, M. R. Guelfi, and G. F. Gensini, “Darknet and bitcoin, the obscure and anonymous side of the internet in healthcare,” *Technology and Health Care*, vol. 24, no. 6, pp. 969–972, 2016.

[38] R. S. Portnoff, D. Y. Huang, P. Doerfler, S. Afroz, and D. McCoy, “Backpage and bitcoin: Uncovering human traffickers,” in *KDD*, 2017, pp. 1595–1604.

[39] J. E. Hopcroft and R. M. Karp, “An nˆ5/2 algorithm for maximum matchings in bipartite graphs,” *SIAM Journal on computing*, vol. 2, no. 4, pp. 225–231, 1973.

[40] J. Edmonds, “Maximum matching and a polyhedron with 0, 1-vertices,” *Journal of research of the National Bureau of Standards B*, vol. 69, no. 125-130, pp. 55–56, 1965.

[41] R. Jonker and T. Volgenant, “Improving the hungarian assignment algorithm,” *Operations Research Letters*, vol. 5, no. 4, pp. 171–175, 1986.

[42] A. Krause and D. Golovin, “Submodular function maximization.” 2014.

[43] J. Edmonds, “Submodular functions, matroids, and certain polyhedra,” in *Combinatorial Optimization—Eureka, You Shrink!* Springer, 2003, pp. 11–26.

[44] R. K. Iyer and J. A. Bilmes, “Submodular optimization with submodular cover and submodular knapsack constraints,” in *Advances in Neural Information Processing Systems*, 2013, pp. 2436–2444.

[45] U. Feige, V. S. Mirrokni, and J. Vondrák, “Maximizing non-monotone submodular functions,” *SIAM Journal on Computing*, vol. 40, no. 4, pp. 1133–1153, 2011.

[46] D. Kempe, J. Kleinberg, and É. Tardos, “Maximizing the spread of influence through a social network,” in *KDD*, 2003, pp. 137–146.

[47] J. Leskovec, A. Krause, C. Guestrin, C. Faloutsos, J. VanBriesen, and N. Glance, “Cost-effective outbreak detection in networks,” in *KDD*, 2007, pp. 420–429.

[48] R. M. Karp, “Reducibility among combinatorial problems,” in *Complexity of computer computations*. Springer, 1972, pp. 85–103.

[49] J. L. Bentley and J. H. Friedman, “Data structures for range searching,” *ACM Computing Surveys (CSUR)*, vol. 11, no. 4, pp. 397–409, 1979.

[50] G. L. Nemhauser, L. A. Wolsey, and M. L. Fisher, “An analysis of approximations for maximizing submodular set functions—i,” *Mathematical programming*, vol. 14, no. 1, pp. 265–294, 1978.

[51] F. Iqbal, B. C. Fung, M. Debbabi, R. Batool, and A. Marrington, “Wordnet-based criminal networks mining for cybercrime investigation,” *IEEE Access*, vol. 7, pp. 22 740–22 755, 2019.

[52] F. Iqbal, B. C. Fung, and M. Debbabi, “Mining criminal networks from chat log,” in *2012 IEEE/WIC/ACM International Conferences on Web Intelligence and Intelligent Agent Technology*, vol. 1. IEEE, 2012, pp. 332–337.

[53] T. Anwar and M. Abulaish, “A social graph based text mining framework for chat log investigation,” *Digital Investigation*, vol. 11, no. 4, pp. 349–362, 2014.

[54] D. Van Esch and R. Sproat, “An expanded taxonomy of semiotic classes for text normalization.” in *INTERSPEECH*. Stockholm, 2017, pp. 4016–4020.

[55] M. Chua, D. Van Esch, N. Coccaro, E. Cho, S. Bhandari, and L. Jia, “Text normalization infrastructure that scales to hundreds of language varieties,” in *Proceedings of the eleventh international conference on language resources and evaluation (LREC 2018)*, 2018.

[56] R. Sproat and N. Jaitly, “An rnn model of text normalization.” in *INTERSPEECH*. Stockholm, 2017, pp. 754–758.

[57] M. Elsner and E. Charniak, "You talking to me? a corpus and algorithm for conversation disentanglement," in *Proceedings of ACL-08: HLT*, 2008, pp. 834–842.

[58] J. K. Kummerfeld, S. R. Gouravajhala, J. Peper, V. Athreya, C. Gunasekara, J. Ganhotra, S. S. Patel, L. Polymenakos, and W. S. Lasecki, "A large-scale corpus for conversation disentanglement," *arXiv preprint arXiv:1810.11118*, 2018.

[59] H. Ouchi and Y. Tsuboi, "Addressee and response selection for multi-party conversation," in *Proceedings of the 2016 Conference on Empirical Methods in Natural Language Processing*, 2016, pp. 2133–2143.

[60] J. Kauttonen and L. Aunimo, "Dialog modelling experiments with finnish one-to-one chat data," in *Conference on Artificial Intelligence and Natural Language.* Springer, 2020, pp. 34–53.

[61] H. Dong, S. C. Hui, and Y. He, "Structural analysis of chat messages for topic detection," *Online Information Review*, 2006.

[62] P. Mutton, "Inferring and visualizing social networks on internet relay chat," in *Proceedings. Eighth International Conference on Information Visualisation, 2004. IV 2004.* IEEE, 2004, pp. 35–43.

[63] D. Rosen, V. Miagkikh, and D. Suthers, "Social and semantic network analysis of chat logs," in *Proceedings of the 1st International Conference on Learning Analytics and Knowledge*, 2011, pp. 134–139.

[64] A. G. Hawkes, "Spectra of some self-exciting and mutually exciting point processes," *Biometrika*, vol. 58, no. 1, pp. 83–90, 1971.

[65] M. Eichler, R. Dahlhaus, and J. Dueck, "Graphical modeling for multivariate hawkes processes with nonparametric link functions," *Journal of Time Series Analysis*, vol. 38, no. 2, pp. 225–242, 2017.

[66] K. Zhou, H. Zha, and L. Song, "Learning social infectivity in sparse low-rank networks using multi-dimensional hawkes processes," in *Artificial Intelligence and Statistics*. PMLR, 2013, pp. 641–649.

[67] ——, "Learning triggering kernels for multi-dimensional hawkes processes," in *International Conference on Machine Learning*. PMLR, 2013, pp. 1301–1309.

[68] H. Xu, M. Farajtabar, and H. Zha, "Learning granger causality for hawkes processes," in *International Conference on Machine Learning*. PMLR, 2016, pp. 1717–1726.

[69] H. Xu, W. Wu, S. Nemati, and H. Zha, "Patient flow prediction via discriminative learning of mutually-correcting processes," *IEEE transactions on Knowledge and Data Engineering*, vol. 29, no. 1, pp. 157–171, 2016.

[70] S. Zhu and Y. Xie, "Spatial-temporal-textual point processes with applications in crime linkage detection," *arXiv preprint arXiv:1902.00440*, 2019.

[71] A. Veen and F. P. Schoenberg, "Estimation of space–time branching process models in seismology using an em–type algorithm," *Journal of the American Statistical Association*, vol. 103, no. 482, pp. 614–624, 2008.

[72] Y. Ogata, "Statistical models for earthquake occurrences and residual analysis for point processes," *Journal of the American Statistical association*, vol. 83, no. 401, pp. 9–27, 1988.

[73] S. J. Hardiman, N. Bercot, and J.-P. Bouchaud, "Critical reflexivity in financial markets: a hawkes process analysis," *The European Physical Journal B*, vol. 86, no. 10, pp. 1–9, 2013.

[74] S. Linderman and R. Adams, "Discovering latent network structure in point process data," in *International Conference on Machine Learning*. PMLR, 2014, pp. 1413–1421.

[75] E. Choi, N. Du, R. Chen, L. Song, and J. Sun, "Constructing disease network and temporal progression model via context-sensitive hawkes process," in *2015 IEEE International Conference on Data Mining*. IEEE, 2015, pp. 721–726.

[76] S. W. Linderman and R. P. Adams, "Scalable bayesian inference for excitatory point process networks," *arXiv preprint arXiv:1507.03228*, 2015.

[77] H. Xu, D. Luo, and H. Zha, "Learning hawkes processes from short doubly-censored event sequences," in *International Conference on Machine Learning*. PMLR, 2017, pp. 3831–3840.

[78] H. Xu and H. Zha, "A dirichlet mixture model of hawkes processes for event sequence clustering," *arXiv preprint arXiv:1701.09177*, 2017.

[79] J. Devlin, M.-W. Chang, K. Lee, and K. Toutanova, "Bert: Pre-training of deep bidirectional transformers for language understanding," *arXiv preprint arXiv:1810.04805*, 2018.

[80] A. Simma and M. I. Jordan, "Modeling events with cascades of poisson processes," *arXiv preprint arXiv:1203.3516*, 2012.

[81] Z. Yang, Z. Dai, Y. Yang, J. Carbonell, R. R. Salakhutdinov, and Q. V. Le, "Xlnet: Generalized autoregressive pretraining for language understanding," *Advances in neural information processing systems*, vol. 32, 2019.

[82] E. M. Smith, M. Williamson, K. Shuster, J. Weston, and Y.-L. Boureau, "Can you put it all together: Evaluating conversational agents' ability to blend skills," *arXiv preprint arXiv:2004.08449*, 2020.

[83] K. Zhou, S. Prabhumoye, and A. W. Black, "A dataset for document grounded conversations," *arXiv preprint arXiv:1809.07358*, 2018.

[84] K. Yoshino, C. Hori, J. Perez, L. F. D'Haro, L. Polymenakos, C. Gunasekara, W. S. Lasecki, J. K. Kummerfeld, M. Galley, C. Brockett *et al.*, "Dialog system technology challenge 7," *arXiv preprint arXiv:1901.03461*, 2019.

[85] S. Zhang, E. Dinan, J. Urbanek, A. Szlam, D. Kiela, and J. Weston, "Personalizing dialogue agents: I have a dog, do you have pets too?" *arXiv preprint arXiv:1801.07243*, 2018.

[86] Y. Chen, "Thinning algorithms for simulating point processes," *Florida State University, Tallahassee, FL*, 2016.

[87] T. Sutikno, L. Handayani, D. Stiawan, M. A. Riyadi, and I. M. I. Subroto, "Whatsapp, viber and telegram: Which is the best for instant messaging?" *International Journal of Electrical & Computer Engineering (2088-8708)*, vol. 6, no. 3, 2016.

[88] , "Telegram: the mighty application that isis loves," *:* , no. 3 (25), pp. 198–200, 2017.

[89] M. N. Yusoff, A. Dehghantanha, and R. Mahmod, "Forensic investigation of social media and instant messaging services in firefox os: Facebook, twitter, google+, telegram, openwapp, and line as case studies," in *Contemporary digital forensic investigations of cloud and mobile applications.* Elsevier, 2017, pp. 41–62.

[90] N. Christin, "Traveling the silk road: A measurement analysis of a large anonymous online marketplace," in *Proceedings of the 22nd international conference on World Wide Web*, 2013, pp. 213–224.

[91] C. Anglano, M. Canonico, and M. Guazzone, "Forensic analysis of telegram messenger on android smartphones," *Digital Investigation*, vol. 23, pp. 31–49, 2017.

[92] G. B. Satrya, P. T. Daely, and M. A. Nugroho, "Digital forensic analysis of telegram messenger on android devices," in *2016 International Conference on Information & Communication Technology and Systems (ICTS).* IEEE, 2016, pp. 1–7.

[93] J. Gregorio, A. Gardel, and B. Alarcos, “Forensic analysis of telegram messenger for windows phone,” *Digital Investigation*, vol. 22, pp. 88–106, 2017.

[94] Z. Yue, Y. Wang, J. Duan, T. Yang, C. Huang, Y. Tong, and B. Xu, “Ts2vec: Towards universal representation of time series,” *arXiv preprint arXiv:2106.10466*, 2021.

[95] Q. Lei, J. Yi, R. Vaculin, L. Wu, and I. S. Dhillon, “Similarity preserving representation learning for time series clustering,” *arXiv preprint arXiv:1702.03584*, 2017.

[96] E. Eldele, M. Ragab, Z. Chen, M. Wu, C. K. Kwoh, X. Li, and C. Guan, “Time-series representation learning via temporal and contextual contrasting,” *arXiv preprint arXiv:2106.14112*, 2021.

[97] F. Chen, Y.-C. Wang, B. Wang, and C.-C. J. Kuo, “Graph representation learning: a survey,” *APSIPA Transactions on Signal and Information Processing*, vol. 9, 2020.

[98] I. T. Jolliffe and J. Cadima, “Principal component analysis: a review and recent developments,” *Philosophical Transactions of the Royal Society A: Mathematical, Physical and Engineering Sciences*, vol. 374, no. 2065, p. 20150202, 2016.

[99] J. Ye, R. Janardan, and Q. Li, “Two-dimensional linear discriminant analysis,‖ in advances in neural information processing systems, vol. 17,” 2005.

[100] S. L. Robinson and R. J. Bennett, “A typology of deviant workplace behaviors: A multidimensional scaling study,” *Academy of management journal*, vol. 38, no. 2, pp. 555–572, 1995.

[101] O. Samko, A. D. Marshall, and P. L. Rosin, “Selection of the optimal parameter value for the isomap algorithm,” *Pattern Recognition Letters*, vol. 27, no. 9, pp. 968–979, 2006.

[102] S. T. Roweis and L. K. Saul, “Nonlinear dimensionality reduction by locally linear embedding,” *science*, vol. 290, no. 5500, pp. 2323–2326, 2000.

[103] M. T. Harandi, C. Sanderson, S. Shirazi, and B. C. Lovell, "Graph embedding discriminant analysis on grassmannian manifolds for improved image set matching," in *CVPR 2011*. IEEE, 2011, pp. 2705–2712.

[104] B. Perozzi, R. Al-Rfou, and S. Skiena, "Deepwalk: Online learning of social representations," in *Proceedings of the 20th ACM SIGKDD international conference on Knowledge discovery and data mining*, 2014, pp. 701–710.

[105] A. Grover and J. Leskovec, "node2vec: Scalable feature learning for networks," in *Proceedings of the 22nd ACM SIGKDD international conference on Knowledge discovery and data mining*, 2016, pp. 855–864.

[106] Y. Wang, H. Yao, and S. Zhao, "Auto-encoder based dimensionality reduction," *Neurocomputing*, vol. 184, pp. 232–242, 2016.

[107] H.-C. Shin, H. R. Roth, M. Gao, L. Lu, Z. Xu, I. Nogues, J. Yao, D. Mollura, and R. M. Summers, "Deep convolutional neural networks for computer-aided detection: Cnn architectures, dataset characteristics and transfer learning," *IEEE transactions on medical imaging*, vol. 35, no. 5, pp. 1285–1298, 2016.

[108] A. Krizhevsky, I. Sutskever, and G. E. Hinton, "Imagenet classification with deep convolutional neural networks," *Advances in neural information processing systems*, vol. 25, 2012.

[109] X. Li, Y. Wu, M. Ester, B. Kao, X. Wang, and Y. Zheng, "Semi-supervised clustering in attributed heterogeneous information networks," in *Proceedings of the 26th international conference on world wide web*, 2017, pp. 1621–1629.

[110] Y. Zhang, Y. Fan, W. Song, S. Hou, Y. Ye, X. Li, L. Zhao, C. Shi, J. Wang, and Q. Xiong, "Your style your identity: Leveraging writing and photography styles for drug trafficker identification in darknet markets over attributed heterogeneous information network," in *The World Wide Web Conference*, 2019, pp. 3448–3454.

[111] Y. Sun, J. Han, X. Yan, P. S. Yu, and T. Wu, "Pathsim: Meta path-based top-k similarity search in heterogeneous information networks," *Proceedings of the VLDB Endowment*, vol. 4, no. 11, pp. 992–1003, 2011.

[112] Y. Dong, N. V. Chawla, and A. Swami, "metapath2vec: Scalable representation learning for heterogeneous networks," in *Proceedings of the 23rd ACM SIGKDD international conference on knowledge discovery and data mining*, 2017, pp. 135–144.

[113] T. Mikolov, I. Sutskever, K. Chen, G. S. Corrado, and J. Dean, "Distributed representations of words and phrases and their compositionality," *Advances in neural information processing systems*, vol. 26, 2013.